

## X-ray Properties of Pre–Main-Sequence Stars in the Orion Nebula Cluster with Known Rotation Periods

Keivan G. Stassun<sup>2</sup>, David R. Ardila<sup>3</sup>, Mary Barsony<sup>4</sup>, Gibor Basri<sup>5</sup>, and Robert D. Mathieu<sup>6</sup>

### ABSTRACT

We re-analyze all archival *Chandra/ACIS* observations of the Orion Nebula Cluster (ONC) to study the X-ray properties of a large sample of pre–main-sequence (PMS) stars with optically determined rotation periods. Our goal is to elucidate the origins of X-rays in PMS stars by seeking out connections between the X-rays and the mechanisms most likely driving their production—rotation and accretion. Stars in our sample have  $L_X/L_{bol}$  near, but below, the “saturation” value of  $10^{-3}$ . In addition, in this sample X-ray luminosity is significantly correlated with stellar rotation, in the sense of *decreasing*  $L_X/L_{bol}$  with more rapid rotation. These findings suggest that stars with optical rotation periods are in the “super-saturated” regime of the rotation-activity relationship, consistent with their Rossby numbers. However, we also find that stars with optical rotation periods are significantly biased to high  $L_X$ . This is not the result of magnitude bias in the optical rotation-period sample but rather to the diminishingly small amplitude of optical variations in stars with low  $L_X$ . Evidently, there exists in the ONC a population of stars whose rotation periods are unknown and that possess lower average X-ray luminosities than those of stars with known rotation periods. These stars may sample the linear regime of the rotation-activity relationship. Accretion also manifests itself in X-rays, though in a somewhat counterintuitive fashion: While stars with spectroscopic signatures of accretion show *harder* X-ray spectra than non-accretors, they show *lower* X-ray luminosities and no enhancement of X-ray variability. We interpret these findings in terms of a common origin for the X-ray emission observed from both accreting and non-accreting stars, with the X-rays from accreting stars simply being attenuated by magnetospheric accretion columns. This suggests that X-rays from PMS stars have their origins primarily in chromospheres, not accretion.

*Subject headings:* stars: pre–main-sequence—stars: X-rays—stars: rotation

---

<sup>2</sup>Department of Physics & Astronomy, Vanderbilt University, Nashville, TN 37235; keivan.stassun@vanderbilt.edu

<sup>3</sup>Johns Hopkins University, Baltimore, MD

<sup>4</sup>San Francisco State University

<sup>5</sup>University of California, Berkeley

<sup>6</sup>University of Wisconsin–Madison

## 1. Introduction

X-rays serve as one of our primary probes of magnetic activity in solar-type stars. Thus, much of our understanding of key physical processes thought to be connected to magnetic fields—stellar winds, for example—derives from the study of stellar X-rays.

One of the most compelling stories in stellar astrophysics told through X-rays is that of the intimate relationship between stellar rotation and magnetic field generation. Indeed, among late-type main-sequence stars, rotation is the strongest correlate of X-ray luminosity, and the observed rotation/X-ray relationship (Pallavicini et al. 1981; Caillault 1996; Randich 1997; Jeffries 1999; Randich 2000) has become central to the current paradigm of dynamo-generated magnetic fields, of magnetically driven stellar winds, and ultimately of the evolution of stellar angular momentum.

The observed relationship between rotation and X-ray emission on the main sequence is remarkably clean, and clearly separates stars into three regimes (cf. Randich (2000)) typically described phenomenologically as the linear, saturated, and super-saturated regimes, in order of increasing stellar rotation (Randich 1997). For slowly rotating stars the X-ray luminosity,  $\log L_X$ , scales linearly with the stellar angular velocity,  $\log \Omega$ , consistent with the theoretical idea that more rapid stellar rotation produces a stronger magnetic field through an  $\alpha - \Omega$ -type dynamo (for stars with radiative cores and convective envelopes) or through a distributed turbulent dynamo (for fully convective stars). For stars rotating more rapidly than a certain threshold, the X-ray luminosity is observed to “saturate” at a fixed value relative to the stellar bolometric luminosity:  $\log L_X/L_{bol} \approx -3$ . While the reasons for saturation have not been well understood, this observation has had important ramifications for efforts to model the angular momentum evolution of young solar-type stars (Krishnamurthi et al. 1997; Bouvier, Forestini, & Allain 1997). The models now routinely include saturation as a key ingredient in their parametrizations of angular momentum evolution through winds. Finally, the most rapidly rotating stars exhibit X-ray emission at levels roughly a factor of 2 below the saturation value. This “super-saturation” effect (James et al. 2000) has been poorly understood. Barnes (2003a,b) has recently re-interpreted super-saturation in terms of a new paradigm for the angular momentum evolution of solar-type stars; whether this new paradigm will survive detailed scrutiny is not yet clear.

What is clear is that the rotation/X-ray relationship serves as a key observational touchstone for developing and evaluating our theoretical understanding of the generation and evolution of stellar magnetic fields, the generation and evolution of stellar winds, and the evolution of stellar angular momentum. Considerable observational effort has been invested, therefore, in trying to establish the presence of a rotation/X-ray relationship among pre-main-sequence (PMS) stars, where the questions of magnetic field generation and evolution, winds, and angular momentum evolution remain largely unanswered. Unfortunately, to date these efforts have not borne much fruit. In one recent study of T Tauri stars (TTS) in Taurus-Auriga (Stelzer & Neuhäuser 2001), a rotation/X-ray correlation has been reported, but the sample size is small ( $N = 39$ ) and there are lingering concerns with respect to completeness/reliability of the rotation periods and biases

in the sample both astrophysical and observational. In particular, as discussed by Feigelson et al. (2003), the Taurus-Auriga PMS population appears to be deficient in both high-mass stars and faint, low-mass weak-lined TTS. In addition, rotation periods in this region were determined from photometric monitoring campaigns some 10 years ago that were relatively sparsely sampled and of relatively short duration, and therefore potentially biased against both very fast and slow rotators.

Two new studies based on deep *Chandra* observations of the Orion Nebula Cluster (ONC) provide the most comprehensive analyses yet of X-rays and rotation in a large, coeval ( $\sim 1$  Myr) sample of PMS stars. Neither the study of Flaccomio and collaborators (Flaccomio et al. 2003; Flaccomio, Micela, & Sciortino 2003a,b) with the High Resolution Camera (HRC), nor that of Feigelson and collaborators (Feigelson et al. 2002, 2003) with the Advanced CCD Imaging Spectrometer (ACIS), found evidence for a rotation/X-ray relationship such as that observed on the main sequence or that reported for Tau-Aur TTS by Stelzer & Neuhäuser (2001). Indeed, these studies find that it is stellar mass that is by far the dominant correlate of PMS X-ray luminosity, with  $\log L_X/L_{bol}$  correlating with rotation either not at all, or perhaps slightly in the opposite sense from the main-sequence rotation/X-ray relationship.

Both studies found that stars with known rotation periods have X-ray luminosities near the main-sequence saturation value of  $\log L_X/L_{bol} \approx -3$ . Moreover, both studies suggest that PMS stars might in fact be *expected* to reside in the super-saturated regime, considering that typical PMS Rossby numbers (Kim & Demarque 1996; Ventura et al. 1998) are small due to the long convective turnover times ( $\tau_c \sim 800$  days) of these very young and fully convective stars. Thus, while direct observation of PMS stars in the linear regime of the rotation/X-ray relationship remains elusive, these studies seem to confirm, if indirectly, the basic picture of the rotation/X-ray relationship by suggesting that all ONC stars are in the super-saturated regime, and that this is where they ought to be.

But not all ONC stars detected by *Chandra* have known rotation periods. To what extent is the sample with periods representative of the entire ONC population in terms of X-ray properties? If they are not representative, how does this group differ in other salient characteristics, such as accretion, and how might these differences affect our interpretation of the origin of X-rays in PMS stars? In addition, while it is clear from previous analyses that X-ray emission from PMS stars is not temporally static—X-ray flaring is ubiquitous in the ONC—it is not yet clear whether or to what extent X-ray variability may be affecting our ability to measure reliable X-ray luminosities. Might X-ray flaring be scrambling the signal of an underlying rotation/X-ray relationship? That some stars flare while others do not is interesting in its own right: Do the flaring characteristics of stars with known rotation periods represent those of all stars? Again, how might differences here affect our interpretation of the origin of PMS X-rays?

Motivated by these questions, we have re-analyzed all archival *Chandra*/ACIS observations of the ONC that include stars with known rotation periods. Our aim is to derive X-ray luminosities for as large a sample of known rotators as possible, employing a consistent analysis scheme throughout,

including filtering of flares in the hopes of minimizing the effects of X-ray variability.

In §2 we describe the data used and our processing/analysis procedures. We then present our basic results in §3, first focusing on the X-ray nature of the rotator sample as compared to the entire ONC population. We show that stars with known rotation periods are significantly more X-ray luminous, and more likely to be X-ray variable, than stars for which rotation periods have not been measured. We then explore the relationship between X-rays and rotation. We find that most stars with known rotation periods appear to be in the super-saturated regime, having  $\log L_X/L_{bol} \lesssim -3$ , with a statistically significant correlation in which faster rotators have lower X-ray luminosities. But we also find that stars without rotation periods—being less X-ray luminous on average—show a range of  $L_X/L_{bol}$  comparable to that observed on the main sequence. These stars may represent the beginnings of the linear regime of the rotation/X-ray relationship. Finally, we explore the relationship between X-rays and accretion. We find that while stars with spectroscopic signatures of accretion show harder X-ray spectra than non-accretors, they also show lower X-ray luminosities and no enhancement of X-ray flaring.

We discuss the implications of our findings in §4, where we (a) emphasize that current rotation-period measurements in the ONC have not probed the full range of underlying stellar X-ray properties, (b) suggest that a main-sequence type relationship between X-rays and rotation may in fact be present in the ONC, and (c) argue that the data imply a chromospheric—not accretion—origin for X-rays from PMS stars. We summarize our conclusions in §5.

## 2. Data

Our primary goal is to study the relationship of stellar X-rays to stellar rotation among a large sample of PMS stars in the ONC. Key parameters in our analysis are the stellar rotation period and the ratio of the X-ray luminosity,  $L_X$ , to the bolometric luminosity,  $L_{bol}$ . We restrict our analysis to observations with ACIS because its energy resolution allows  $L_X$  to be determined from fits to the X-ray spectral energy distribution. We also consider only reasonably long observations ( $\sim 100$  ksec) so that we can attempt to derive quiescent X-ray luminosities by filtering out flaring events.

Thus our study sample comprises ONC stars that: (1) have known rotation periods, (2) have derived bolometric luminosities, and (3) have been observed by the *Chandra* ACIS instrument. Where possible we would also like to study the relationship of X-rays to accretion, so we include such measurements where available.

Here we describe the data from the literature that we compile to form our study sample (§2.1). We also describe the data from the *Chandra* archive that we use (§2.2) as well as the procedures employed in their reduction (§2.2.1) and analysis (§2.2.2). We close with a brief discussion of our assessment of the quality and reliability of the X-ray measurements (§2.2.3).

## 2.1. Supporting data from the literature

Rotation period measurements are available from the optical studies of Stassun et al. (1999) and Herbst et al. (2002) for 431 PMS stars in the ONC which were also included in the optical photometric/spectroscopic study of Hillenbrand (1997). The latter study provides bolometric luminosities and other basic stellar parameters (i.e. masses, effective temperatures, extinctions, etc.) for most (358) of these stars. In addition, the study of Hillenbrand et al. (1998) provides spectroscopic measures of accretion in the form of Ca II equivalent widths. In Table 1 we summarize our study sample, comprising 220 unique stars with rotation periods that we detect in the *Chandra* observations described below. We include relevant stellar properties taken from the sources above.

## 2.2. *Chandra* archival data

There are three ONC observations in the *Chandra* archive relevant to this study, two obtained by Garmire (Obs. ID’s 18 and 1522) and one by Tsujimoto (Obs. ID 634). The Garmire observations are described by Feigelson et al. (2002) and include a 45.3 ksec exposure obtained on 1999 Oct 12–13 and a 37.5 ksec exposure obtained on 2000 Apr 1–2, both centered on the Trapezium. The Tsujimoto observation, described in Tsujimoto et al. (2002), is a single 89.2 ksec exposure centered on the OMC-2/3 region (just North of the Trapezium) obtained on 2000 Jan 1–2.

In all three exposures, the four ACIS-I chips were operational with a total field of view of  $17 \times 17$  arcmin. In addition, all three exposures had the ACIS-S2 chip in operation, which is separated from ACIS-I by 2.7 arcmin and has a field of view of 8.3 arcmin. Finally, the second Garmire exposure included the ACIS-S3 chip, again with a field of view of 8.3 arcmin. We include the ACIS-S data here for completeness, but note that this results in only a few additional sources due to the highly degraded point spread function (PSF) of the instrument at large off-axis angles. The ACIS instrument measures photon arrival times, positions, and energies (0.5–8 keV), so that for each detected source an X-ray light curve and spectral energy distribution can be constructed.

### 2.2.1. Reduction

We reprocessed all three exposures in the same manner, starting from the `_evt1` event files<sup>1</sup>, using the standard CIAO<sup>2</sup> procedure `process_acis_events` and updated calibration files obtained from the *Chandra* X-ray Center<sup>3</sup> (CXC) in Sept 2002. Photon events were filtered according to their grade and status flags, and the images destreaked, following the standard CXC science threads. We

---

<sup>1</sup>Event files consist of arrival times, positions, energies, and other information for each detected X-ray photon.

<sup>2</sup>Chandra Interactive Analysis of Observations (CIAO) version 2.2.

<sup>3</sup>See <http://cxc.harvard.edu>.

also manually updated the astrometric header keywords based on the latest astrometric calibration available from the CXC.

The resulting event files (`_evt2` files) were then searched for point sources using the CIAO task `celldetect`. The task uses a spatially variable PSF, and we kept only those sources with a signal-to-noise ratio (SNR) of 5 or greater. We set the `celldetect` task to return source ellipses with a size of 99% encircled energy, and defined a background annulus whose inner and outer semi-major axes were, respectively, 1.5 and 1.7 times larger than the source ellipse.

To make the photon extraction computationally feasible, at each source position we then extracted a sub-region just larger than the background ellipse, using a set of IDL<sup>4</sup> scripts developed by us. Thus for each of the three exposures, the result of the reduction step is a set of event files, one for each of the detected sources.

### 2.2.2. Analysis

With a set of event files corresponding to each source detected with  $\text{SNR} > 5$ , we next applied an automated time-filtering of each source light curve in order to remove flare events prior to modeling the X-ray spectral energy distribution (SED) to derive X-ray luminosities. The aim of this procedure is to determine a quiescent  $L_X$  for each source. Based on the documented sensitivity limits of ACIS, in all that follows we use only X-ray photons with energies in the range 0.5–8 keV.

The time-filtering of the light curves was implemented in IDL using procedures developed by us. For each source, the process involves the following steps (see example in Fig. 1): (1) Construct source and background light curves using the CIAO `lightcurve` script with a binning interval of 2 ksec; (2) subtract background light curve from source light curve; (3) exclude bins that are  $> 3\sigma$  brighter than the median, which is computed from the lowest 15% of the bins; (4) re-determine the median and again exclude deviant bins, iterating until no more bins are excluded; and (5) output a new event file that includes only the time intervals of the surviving bins.

With time-filtered event files in hand for each of the detected sources, we determined the  $L_X$  of each source via a standard spectral analysis using `SHERPA`. For each source in each of the three exposures, the position-dependent auxiliary response file (ARF) and redistribution matrix file (RMF)<sup>5</sup> were computed with the CIAO `psextract` command and a model spectrum was fit. The model used was a two-component thin thermal plasma with absorption by an intervening column of hydrogen. The free parameters of the model are the absorbing hydrogen column density ( $\log N_H$ ), the temperatures of the two plasma components ( $kT_1$ ,  $kT_2$ ), the metallicity ( $Z$ ), and a

---

<sup>4</sup>Interactive Data Language

<sup>5</sup>The ARF contains the combined telescope/filter/detector areas and efficiencies as a function of energy. The RMF translates detector pulse heights into photon energies.

normalization (scaling) coefficient for each plasma component. A  $\chi^2$  minimization procedure was used to fit each source’s SED for these parameters, iterating until convergence was achieved.

Given the large number of free parameters, there is no guarantee that the best fit adopted is truly a global best fit or even that there is only one possible global best fit. Thus we emphasize that our goal in the spectral fitting is not the values of the model parameters themselves; we simply seek a reasonably good fit from which we can determine the X-ray luminosity of the source. The fit can thus be thought of as a (possibly over-determined) spline fit to the X-ray SED of the source, which we then integrate to measure the source flux,  $F_X$ . Adopting a distance of 470 pc to the ONC we convert the measured  $F_X$  values into  $L_X$ .

In principle, we can correct each  $L_X$  for intervening absorption using the value of  $\log N_H$  determined from the spectral fit. However, Feigelson et al. (2002) have demonstrated that the  $\log N_H$  values determined from spectral fitting do not correspond very well to  $A_V$  values determined from optical photometry/spectroscopy. We thus follow Feigelson et al. (2002) and choose not to correct the measured  $L_X$  for absorption.

With  $L_X$  values determined for each source from each of the three *Chandra* exposures, we match the sources with known rotation periods by searching for a positional match within the error ellipses of the detected X-ray sources. We find 220 stars with rotation periods in the *Chandra* images. In cases where a given target is detected in more than one *Chandra* exposure, we select for our subsequent analysis the *lower* value of  $L_X$ , assuming that the source changed its intrinsic  $L_X$  between observations, and that the lower value represents the best estimate of the quiescent  $L_X$ .

The X-ray properties of these 220 sources (Table 1) are summarized in Table 2, which includes all  $L_X$  measurements of each source (as many as three different measurements because there are three separate exposures). In addition, Table 2 provides the  $L_X$  measurements from Feigelson et al. (2002) for comparison<sup>6</sup>. Those authors detected 253 stars<sup>7</sup> with rotation periods, and here we re-detect 190 of them, presumably due to our higher SNR criterion ( $> 5$ ) for source detection (see above). The 30 stars<sup>8</sup> with rotation periods detected by us and not by Feigelson et al. (2002) (see Table 2) derive from the Tsujimoto et al. (2002) exposure.

Table 2 also includes a descriptor for the variability of each source’s light curve. These are taken from Feigelson et al. (2002) when the source was included in that study; otherwise, the descriptor is assigned by us following the procedure of Feigelson et al. (2002). A designation of ‘Const’ indicates that the light curve shows an approximately constant flux with time; ‘LTVar’

---

<sup>6</sup>We do not include X-ray luminosities derived by Tsujimoto et al. (2002) for comparison as their tabulated values are corrected for extinction, while those reported here and by Feigelson et al. (2002) are not.

<sup>7</sup>The Feigelson et al. (2002) study detected a total of 1075 stars. Included in the *ACIS* field of view were 263 stars with rotation periods; 10 stars with rotation periods were not detected by Feigelson et al. (2002).

<sup>8</sup>Included in the *ACIS* field of view were 35 stars with rotation periods; 5 stars with rotation periods were not detected by us.

indicates statistically significant variability that occurs slowly in time, resulting in a different mean flux level in the different ACIS exposures; ‘Flare’ indicates a statistically significant variation on short timescales; and ‘PosFl’ indicates a flare-like variation of marginal significance. Finally, Table 2 provides a subjective quality flag for each  $L_X$  determination, which we now discuss.

### 2.2.3. Quality assessment

Since our re-reduction of the archival *Chandra* data used updated calibrations, and because our analysis procedures included time-filtering of flares that other authors have not done, in this section we assess the reliability of our reductions. We begin by comparing the  $L_X$  values derived by us to those derived by other authors for the same sources. We then discuss some specific cases in detail in order to illustrate the vagaries inherent to this type of analysis.

To start, we visually inspected the **SHERPA** fit of each source and subjectively flagged those sources whose  $L_X$  values we deemed unreliable due either to an observed spectrum with few counts or to an otherwise poor fit. The result of this procedure is 154 sources whose spectra and corresponding spectral fits we felt were subjectively reasonable. We restrict all subsequent discussion to these 154 sources, which are indicated in Table 2 by a quality flag of ‘1’.

In Fig. 2 we compare the  $L_X$  values obtained by us to those obtained by Feigelson et al. (2002) for the common sources. We basically find good agreement between the two sets of measurements. A gaussian fit to the differences between the two measurements results in a standard deviation of  $\sigma = 0.14$  dex, an offset of 0.15 dex (our measurements being systematically larger), and a small number of outliers.

Approximately 0.04 dex of the systematic offset can be accounted for by the fact that we assume a distance to the ONC of 470 pc while Feigelson et al. (2002) assume a slightly lower value of 450 pc. The remaining difference of 0.1 dex remains unaccounted for, but is not surprising given small differences in the calibrations used in our data reprocessing. On the whole, then, we can report reproducibility of the derived  $L_X$  to a level of  $\sim 0.1$  dex, despite differences in calibration, our time-filtering of flares from the light curves, and so on.

Nonetheless, a few stars have very different  $L_X$  measurements from the two analyses (up to about 1 dex). As an example, we consider star 116, which is the most discrepant between our measurements and that reported by Feigelson et al. (2002). From the two Garmire exposures we measure  $L_X$  values for this source of  $10^{30.7}$  erg/s and  $10^{30.4}$  erg/s, which encouragingly are similar to one another, but are very different from the Feigelson et al. (2002) value of  $10^{29.1}$  erg/s (see Table 2). This is a remarkable difference considering that these values derive from the same photons.

Close inspection of our **SHERPA** fits to the two observations of this source (Fig. 3) do not indicate any obvious problems. Perhaps the discrepancy is the result of our flare filtering procedure. However, the light curve of this source does not include any strong flares and so was not heavily

filtered. In any case, we performed the **SHERPA** analysis once again but on the pre-filtered data from the first Garmire exposure. As expected, the resulting  $L_X$  of  $10^{30.5}$  erg/s differs only slightly from the value we report in Table 2, and the model fit again does not present any obvious problems (Fig. 4). Recalling that the Feigelson et al. (2002) analysis typically used single-component fits to the spectra as compared to our two-component fits, we attempted to reproduce their value by again running the **SHERPA** analysis on the pre-filtered data but this time using only one thermal plasma component to the model fit. The value of  $L_X$  that we derive here ( $10^{30.4}$  erg/s) still does not resolve the discrepancy, and may in fact be a low measure as the model fit in this case underestimates the flux in the two highest energy bins that are not upper limits (Fig. 5).

Thus in this example case, and in the other discrepant cases seen in Fig. 2, we are simply unable to determine the cause of the discrepancy. We provide this exercise as a cautionary lesson about the limits inherent in this type of analysis, but take comfort in the fact that for the majority of the sources used in our analysis the agreement between our values and those derived by Feigelson et al. (2002) is in fact very good.

### 3. Results

The X-ray luminosities for each source in Table 1 resulting from our analysis are given in Table 2, representing 220 stars with known rotation periods that are included in the optical database of Hillenbrand (1997). In this section we report the results for the 154 sources having a quality flag of ‘1’. We remind the reader that our values of  $L_X$  are broadband luminosities over the energy range 0.5 keV to 8 keV, are not corrected for absorption, and do not include photon events that occur during a flare (see §2.2.2). Feigelson et al. (2002) report  $L_X$  measurements for an additional 63 stars with rotation periods detected at lower signal-to-noise; where appropriate we include these measurements in our analysis and discussion, but in all cases we maintain a distinction between this larger sample and the subset which we believe to be of highest quality.

We begin by presenting the basic X-ray properties of these sources, emphasizing two biases that appear to be inherent to PMS stars having measurable rotation periods (§3.1), namely, a tendency toward higher X-ray luminosities (§3.1.1) and toward higher levels of X-ray variability (§3.1.2). With these biases in mind, we next examine the X-ray data vis-a-vis rotation (§3.2) and accretion (§3.3) for clues into the possible mechanisms for X-ray production in these stars.

#### 3.1. Basic X-ray properties of stars with known rotation periods

In this section we discuss the basic X-ray properties—luminosity and variability—of stars with known rotation periods. By comparing these properties to those of other stars detected in the *Chandra* observations, we find two biases—astrophysical in origin—in the rotation-period sample. Stars with measured rotation periods are: (1) more X-ray luminous both absolutely (i.e.

$L_X$ ) and relative to the stellar bolometric luminosity (i.e.  $L_X/L_{bol}$ ); and (2) more likely to be X-ray variable than are stars in the overall PMS population of the ONC. These results are highly statistically significant. We emphasize that these biases are not due to observational bias (e.g., optical magnitude bias) in the rotation-period sample, and are therefore likely to have a physical basis as we discuss in §4.1. Here we present the evidence for these two biases in turn.

### 3.1.1. Bias: X-ray luminosity

We find that ONC stars with known rotation periods are significantly biased to high X-ray luminosities. In Fig. 6 we plot both the distribution of  $\log L_X$  for our study sample (Table 2; hatched histogram) as well as the larger sample of stars with rotation periods detected by Feigelson et al. (2002) (dashed histogram). For comparison, the solid histogram shows the distribution of  $\log L_X$  for all stars reported by Feigelson et al. (2002) included in the optical survey of Hillenbrand (1997). To demonstrate that the bias to high  $L_X$  among stars with rotation periods is not due to optical bias in the rotation-period studies, we include here only those stars detected by Feigelson et al. (2002) having optical magnitudes bright enough ( $I \lesssim 17$ ) to have been included in the optical samples studied for rotation periods (Stassun et al. 1999; Herbst et al. 2002). We further restrict this comparison sample to only stars with masses  $M < 3 M_\odot$ , as this represents the range of stellar masses among stars with rotation period measurements.

While the stars with known rotation periods (dashed histogram) exhibit a range of  $L_X$ , this range is  $\sim 0.5$  dex smaller than that spanned by the underlying ONC population (solid histogram). Moreover, the  $L_X$  distribution of these stars is skewed with respect to the overall distribution, such that stars with rotation periods exhibit higher average  $L_X$ . To show this more clearly, the distribution of  $L_X$  for stars *without* rotation periods (i.e. the difference between the solid and dashed histograms) is shown also (dot-dashed histogram).

A two-sided K-S test indicates that the probability of the  $L_X$  distributions for stars with and without rotation periods (dashed and dot-dashed histograms) being drawn from the same parent population is  $7 \times 10^{-7}$ . In addition, a Student’s  $t$  test gives a probability of only  $2 \times 10^{-10}$  that the means of these two distributions ( $\log L_X = 29.75$  erg/s for stars with rotation periods and  $\log L_X = 29.39$  erg/s for stars without) are the same.

A similar result is obtained when we consider  $L_X/L_{bol}$  instead of  $L_X$  (Fig. 7). Here, a two-sided K-S test gives a probability of  $2 \times 10^{-8}$  that the  $L_X/L_{bol}$  distributions for stars with and without rotation periods are drawn from the same parent population. And a Student’s  $t$  test gives a probability of  $6 \times 10^{-10}$  that the means of these two distributions ( $\log L_X/L_{bol} = -3.67$  for stars with rotation periods and  $\log L_X/L_{bol} = -4.09$  for stars without) are the same.

### 3.1.2. Bias: X-ray variability

A similar bias manifests itself with respect to X-ray variability of the sources. The subset of stars in our sample whose X-ray light curves are variable (‘Flare’, ‘PosFl’, or ‘LTVar’ in Table 2) comprise  $82\% \pm 3\%$  of our study sample (uncertainties determined from the binomial distribution). Similarly,  $70\% \pm 3\%$  of stars with rotation periods in the larger sample of Feigelson et al. (2002) show variability. In comparison, a smaller fraction,  $57\% \pm 2\%$ , of ONC stars in the Feigelson et al. (2002) study that lack rotation periods show such variability.

For the entire sample of stars with rotation periods, this difference in X-ray variability is statistically significant. A  $\chi^2$  test gives a probability of 0.001 that stars with and without rotation periods have equal occurrences of variability. For our high-quality sample, where the signal-to-noise is higher and variability in the light curves is therefore better determined, a  $\chi^2$  test gives a probability of  $2 \times 10^{-9}$  that the occurrence of variability is the same as that found among stars without rotation periods.

There thus appears to be significant evidence for an enhancement of X-ray variability among stars in the ONC with rotation periods, particularly when we restrict our analysis to those stars with the highest quality X-ray light curves.

## 3.2. Rotation

X-ray emission on the main sequence among stars with  $M \lesssim 3 M_{\odot}$  is believed to be driven by stellar rotation, and this results in a clear, observable correlation between stellar rotation and X-ray luminosity. The relationship between X-ray luminosity and stellar rotation period for our study sample is shown in Fig. 8, where we plot  $\log L_X/L_{bol}$  vs.  $\log P_{rot}$ . For ease of comparison, the vertical scale is set to the full range of  $\log L_X/L_{bol}$  observed on the main sequence.

As noted above and in the previous studies of Flaccomio, Micela, & Sciortino (2003a) and Feigelson et al. (2003), these stars show a mean  $\log L_X/L_{bol}$  near the main sequence saturation value of  $-3$ , though somewhat lower (mean  $\log L_X/L_{bol} = -3.67$  for all stars with rotation periods). Taken at face value, these data present no clear evidence for an X-ray/rotation relationship of the sort seen on the main sequence.

At a more detailed level, these data provide possible evidence for these stars being in the super-saturated regime of the rotation/X-ray relationship. In addition to having a mean  $L_X/L_{bol}$  below the saturation value, the data in Fig. 8 also show a weak, but statistically significant, trend of increasing  $L_X/L_{bol}$  with increasing rotation period, as might be expected for stars in the super-saturated regime. Among all stars with rotation periods, a Spearman’s  $\rho$  rank-correlation test gives a probability of  $9 \times 10^{-4}$  that  $P_{rot}$  is uncorrelated with  $L_X/L_{bol}$ . The same trend is present among the smaller set of stars detected in this study, though only at 95% significance.

To effect a better comparison with super-saturation on the main sequence, we transform the abscissa from  $P_{rot}$  to Rossby number,  $R_0$ , defined as the ratio between  $P_{rot}$  and the convective turnover timescale,  $\tau_c$ <sup>9</sup>, which is typically used to show the X-ray/rotation relationship on the main sequence. This is shown in Fig. 9, where the solid line represents the main-sequence relationship as determined by Pizzolato et al. (2003), and where the stars in our sample now appear explicitly in the super-saturated regime.

Fig. 9 also shows the  $\log L_X/L_{bol}$  for the remainder of the ONC sample from Feigelson et al. (2002) with  $M < 3 M_\odot$  (crosses plotted arbitrarily at  $\log R_0 = 0$ ; these are the same stars as in the dot-dashed histogram in Fig. 7). As we have seen (§3.1.1, Figs. 6 and 7), these stars are on average less X-ray luminous than are stars with known rotation periods. Might there also be differences on average in their rotational properties?

For 40 of these stars lacking optical rotation periods,  $v \sin i$  measurements are available from the study of Rhode, Herbst, & Mathieu (2001), allowing us to infer their (projected) rotational characteristics. In Fig. 10 we show the  $L_X$  distribution for these stars segregated into two groups, fast (11 stars) and slow rotators (29 stars), defined on the basis of whether Rhode, Herbst, & Mathieu (2001) report a  $v \sin i$  measurement or a  $v \sin i$  upper limit (i.e. whether the spectral lines are broadened beyond the instrumental resolution or not). The slow rotators indeed appear to be skewed to lower  $L_X$ , and both a two-sided K-S test and a Student’s  $t$  test confirm this at the 99% confidence level. The difference between slow and rapid rotators is not statistically significant when we consider  $L_X/L_{bol}$  instead of  $L_X$ .

A similar test is possible among stars with  $v \sin i$  measurements that *do* have rotation periods (58 fast and 62 slow rotators). The  $L_X$  distributions of these two groups are statistically indistinguishable. Apparently, the difference in  $L_X$  between fast and slow rotators is only present among stars lacking optical rotation periods.

Thus, while there is not a one-to-one correlation between  $L_X$  and  $v \sin i$  for stars without optical rotation periods, there is a marginally significant tendency for the X-ray faint stars in this group to also have slower rotation speeds. This is in the opposite sense to what we find above for stars that do have optical rotation periods, in which the X-ray luminosity *increases* with slower rotation similar to super-saturated stars on the main sequence (cf. Fig. 9 in Pizzolato et al. (2003)), albeit with a large scatter.

---

<sup>9</sup>The convective turnover timescale,  $\tau_c$ , is typically determined from stellar interiors models for stars of the appropriate mass and age. As discussed by Flaccomio (2002), at the young age of the ONC the value of  $\tau_c$  is roughly constant for these fully convective low-mass stars. We thus convert  $P_{rot}$  to  $R_0$  by scaling the former by a constant value of  $\tau_c = 800$  days (Ventura et al. 1998).

### 3.3. Accretion

Accretion is another mechanism possibly related to X-ray production in PMS stars, and indeed accretion appears to manifest itself strongly in the X-ray properties of the stars in our study. We use the strength of emission in the Ca II line as measured by Hillenbrand et al. (1998) to determine which stars are actively accreting: Following Flaccomio, Micela, & Sciortino (2003a) we take stars with Ca II equivalent widths (EW) of  $< -1 \text{ \AA}$  (i.e. in emission) to be those actively accreting, while those with  $\text{EW} > 1 \text{ \AA}$  (i.e. in absorption) to be non-accreting.

Ca II EW measurements are available for 117 stars in our sample and for 199 stars among all stars with rotation periods. In light of the biases inherent to the rotation period sample noted in §3.1, where appropriate we also explore accretion signatures in the full sample of ONC stars from the study of Feigelson et al. (2002).

We find that stars with active accretion signatures in Ca II, while no more likely to show X-ray flares than non-accreting stars, are systematically less X-ray luminous and exhibit systematically harder X-ray spectra. We discuss in turn the relationship between accretion and X-ray flaring, X-ray luminosity, and X-ray hardness.

#### 3.3.1. Accretion and X-ray flaring

We begin by noting that spectroscopic signatures of active accretion are relatively rare among the stars in our sample. Among the 117 stars from this study that have Ca II measurements, only 10 stars show Ca II clearly in emission (i.e.  $\text{EW} < -1 \text{ \AA}$ ), whereas 66 stars show Ca II clearly in absorption (i.e.  $\text{EW} > 1 \text{ \AA}$ ). Among those few stars that do show evidence for active accretion, all 10 of them exhibit X-ray flaring in the *Chandra* data (‘Flare’ or ‘PosFl’ in Table 2). Among the non-accreting stars, 70% (46/66 stars) show such evidence for X-ray flaring. Because of the small number of accreting sources in this sample, this difference is not statistically significant.

Similarly, among the larger sample of all stars with rotation periods only 28/199 stars show Ca II clearly in emission, whereas 77 stars show Ca II in absorption. Among the 28 accreting stars, 15 (54%) show evidence for X-ray flaring, while among the non-accreting stars 47 stars (61%) do. This small difference is not statistically significant.

Considering the entire ONC sample included in the study of Feigelson et al. (2002), there are 254 stars for which Hillenbrand et al. (1998) report a Ca II EW of either  $< -1 \text{ \AA}$  (126 stars) or  $> 1 \text{ \AA}$  (128 stars). In this larger sample, 41% of the accreting stars show X-ray flaring, and 48% of the non-accreting stars do, again indicating no relationship between accretion and X-ray flaring.

We thus find that while stars with optical rotation periods are predominantly non-accreting (see also Stassun et al. (1999); Herbst et al. (2002)), X-ray flaring is nonetheless ubiquitous among them (§3.1.2), and the presence of active accretion does not significantly enhance this X-ray flaring.

### 3.3.2. Accretion and X-ray luminosity

Among the stars with measured rotation periods, we find a hint that actively accreting stars have lower X-ray luminosities than their non-accreting counterparts. As above, there are only 28 stars with rotation periods that show clear signs of active accretion and 77 stars that clearly do not. Comparing the  $L_X$  distributions of these two subsets, a Student’s  $t$  test reveals different means—with accretors being less luminous—at 98% confidence.

However, within the full ONC sample we find that this difference in  $L_X$  between accretors and non-accretors is highly statistically significant. Of the 529 stars from Hillenbrand et al. (1998) in the *ACIS* field, Feigelson et al. (2003) detect 525 stars with  $M < 3 M_\odot$ . Of these, 256 have  $\text{EW}(\text{Ca II}) < -1 \text{ \AA}$  (126 detected in X-rays, 0 undetected) or  $\text{EW}(\text{Ca II}) > 1 \text{ \AA}$  (128 detected in X-rays, 2 undetected). Here we ignore the two undetected stars. As Fig. 11a shows, the  $L_X$  distributions of accretors and non-accretors are clearly different; a two-sided K-S test reveals that the probability that the two are drawn from the same parent distribution is  $3 \times 10^{-5}$ .

As demonstrated by Feigelson et al. (2002) and Flaccomio et al. (2003),  $L_X$  correlates strongly with stellar mass. Thus, the differences in  $L_X$  among accretors and non-accretors might be the result of a correlation between accretion and stellar mass. Fig. 11b shows the  $L_X$  distributions for accretors and non-accretors as a function of mass (stellar masses taken from Feigelson et al. (2002)). The center of each box marks the position of the median  $L_X$  in that mass bin. If the indented regions around the medians (“notches”) of two boxes do not overlap, the medians are different with  $> 95\%$  confidence (see Feigelson et al. (2003) for an explanation of box plots). We see that for stars below  $\sim 0.5 M_\odot$ , those with spectroscopic accretion indicators have significantly lower  $L_X$  than stars that do not have spectroscopic accretion indicators. The number of objects in the higher mass bins, particularly those showing active accretion in Ca II, is sufficiently small that the uncertainties on the boxes in Fig. 11b are large and any differences between accretors and non-accretors may be difficult to detect.

### 3.3.3. Accretion and X-ray hardness

In addition to X-ray luminosity, the *Chandra/ACIS* data allow us to compare accretors and non-accretors in terms of X-ray spectral properties. Fig. 12a compares the histograms of hardness ratios [ $\text{HR} = (L_h - L_s)/(L_h + L_s)$ ] for accretors and non-accretors, where  $L_s$  is the X-ray luminosity from 0.5 to 2 keV, and  $L_h$  is the X-ray luminosity from 2 to 8 keV. As above, we include in our analysis all ONC stars from the study of Feigelson et al. (2002) with  $M < 3 M_\odot$ .

We find that accretors exhibit systematically harder X-ray spectra than non-accretors, and the likelihood of both samples being drawn from the same parent distribution is  $10^{-5}$ . Fig. 12b shows the mass dependence of the HR. Similar to Fig. 11b, a difference between accretors and non-accretors is clear for stars with masses below  $\sim 0.5 M_\odot$ .

## 4. Discussion

From our analysis of all archival *Chandra/ACIS* observations of a large sample of PMS stars in the ONC, we have identified important biases in the basic X-ray characteristics (luminosity and variability) of stars with optically determined rotation periods as compared to the overall population of PMS stars detected by *Chandra*. In addition, we have explored possible relationships between the X-rays observed from these stars and the two physical mechanisms most likely responsible for their production: rotation and accretion.

In this section we explore in greater depth the implications of the findings presented in §3 toward the goal of further elucidating the origin of X-rays in PMS stars. We structure this discussion again around the two central physical mechanisms of rotation and accretion. We will argue that the data hint at the presence of an underlying rotation/X-ray relationship qualitatively similar to that observed on the main sequence, and we will show that the observed differences in X-ray characteristics between accretors and non-accretors are in fact consistent with a picture in which all stars have intrinsically similar X-ray emission properties. We therefore posit that rotation and not accretion is primarily responsible for the production of X-rays in PMS stars at  $\sim 1$  Myr.

### 4.1. Rotation

In seeking to find a rotation/X-ray relationship among PMS stars analogous to that observed on the main sequence, it is logical to focus on the X-ray properties of PMS stars with known rotation periods. Unfortunately, the full rotation/X-ray relationship, if it exists among PMS stars in the ONC, might not be discernable from those stars with optically determined rotation periods alone. As we have seen, these stars are significantly biased to higher values of  $L_X$  (and  $L_X/L_{bol}$ ) than are stars without rotation periods. These stars may therefore only allow us to probe the super-saturated regime of any underlying rotation/X-ray relationship.

Why are PMS stars with optically determined rotation periods biased in their basic X-ray characteristics? It appears that this bias results from the fact that rotation periods can only be measured among stars with spots that are sufficiently large and long-lived to produce stable periodic signals in the optical.

To show this, in Fig. 13a we plot the amplitude of optical variability,  $\Delta I$ , as reported by Herbst et al. (2002) for PMS stars in the ONC with rotation periods, against these stars' X-ray luminosities as determined in this study and in the study of Feigelson et al. (2002). The two quantities are highly correlated. Whether we consider all stars with rotation periods, or only those detected in this study (filled circles in Fig. 13), a Spearman's rank-correlation analysis yields a probability of  $\sim 10^{-4}$  that  $\Delta I$  and  $L_X$  are uncorrelated. The same result is obtained when we consider  $L_X/L_{bol}$  instead of  $L_X$  (Fig. 13b). In this case, we find a correlation at marginal confidence (99%) when we consider only the stars from this study, but a probability of  $1 \times 10^{-6}$  that the two quantities are uncorrelated

when we include all stars with rotation periods.

The implication is that we do not observe stars with rotation periods at very low  $L_X$  because the amplitude of photometric variability in the optical becomes diminishingly small, ultimately smaller than the minimum signal detectable ( $\Delta I \sim 0.03$  mag) by existing rotation-period studies of the ONC (Stassun et al. 1999; Herbst et al. 2002).

In light of the fact that stars with rotation periods have high X-ray luminosities, it is perhaps not surprising that these stars appear to be in the super-saturated regime. But if these stars are indeed super-saturated as Fig. 9 implies, then the optical variability data would seem to imply a qualitatively different picture for the surfaces of super-saturated stars than that commonly assumed. The mental image often invoked in the context of saturation is that of a star whose surface has become completely threaded by magnetic flux tubes, resulting in spot coverage fractions approaching unity. Yet in Fig. 13 there are stars at both low and high  $L_X/L_{bol}$  that show relatively small amplitudes of optical variability, suggesting that spot coverage among many of these “super-saturated” stars is relatively light.

On the other hand, Fig. 13 may be telling us that these stars do indeed have spots covering large fractions of their surfaces, but that we are seeing changes in the magnetic topologies of these stars as a function of  $L_X/L_{bol}$ . For example, stars at lower  $L_X/L_{bol}$  may represent stars with relatively disorganized surface fields that produce relatively small spots more-or-less uniformly distributed on the stellar surface. Such small, uniformly distributed spots would produce only low-amplitude variability in the optical even if they cover a large fraction of the stellar surface. In contrast, stars with larger  $L_X/L_{bol}$  could represent cases where the magnetic field has become more coherently organized into relatively large spots that are distributed more asymmetrically on the stellar surface, thereby giving rise to larger photometric variability in the optical. That not all stars with large  $L_X/L_{bol}$  have correspondingly large  $\Delta I$  is perhaps simply due to geometrical effects (varying spot sizes/temperatures, spot latitudes, inclination angles, etc.), or it may suggest that strong magnetic fields do not instantaneously arrange into organized configurations.

This interpretation is similar to that proposed by Barnes (2003b), who argues that stars in the super-saturated regime are cases in which the stellar magnetic field has not yet become sufficiently organized to couple the stellar interior to the surface, and therefore the star’s rotation is not effectively braked. Barnes (2003b) further argues that as the stellar magnetic field becomes more organized and achieves maximum strength, it becomes more deeply rooted, the X-ray luminosity also reaches maximum strength (saturation), and magnetic braking begins to affect the entire star. In this way, Barnes (2003b) offers a possible explanation for the positive correlation observed between  $P_{rot}$  and  $L_X/L_{bol}$  among stars in the super-saturated regime. These are speculative ideas to be sure; our aim here is to provide additional observational fodder to the question of what super-saturation is really telling us about the magnetic nature of PMS stars.

At any rate, if we accept the inference that stars in the ONC with rotation periods do represent the super-saturated regime of the rotation/X-ray relationship, then the question arises whether

there is evidence for an unseen linear regime in the rotation/X-ray relationship. Fig. 9 tells us that there are indeed stars with sufficiently low  $L_X/L_{bol}$ , but do these stars also rotate more slowly? While the available  $v \sin i$  data do not show a one-to-one relationship between  $v \sin i$  and  $L_X$ , we do find evidence that slower rotators do indeed have lower  $L_X$  (§3.2), hinting at behavior qualitatively consistent with the linear regime of the rotation/X-ray relationship.

Thus, a picture begins to emerge from the data in which X-ray luminosity does appear to be related to stellar rotation among PMS stars in the ONC. Stars with rotation periods, biased as they are in  $L_X$ , may represent the super-saturated and saturated regimes, and some stars lacking rotation periods may represent the saturated and (at least part of) the linear regime, implying a population of very slow rotators among these stars.

An alternative to the slow-rotator explanation for the lower  $L_X$  of stars without rotation periods is that stars without rotation periods are predominantly active accretors, and that it is accretion that is acting to suppress the  $L_X$  of these stars (see §3.3.2). Indeed, among the sample of stars from Feigelson et al. (2002) that lack rotation periods, those with spectroscopic signatures of active accretion (i.e.  $\text{EW}(\text{Ca II}) \leq -1 \text{ \AA}$ ) outnumber those without such signatures by 2:1. To examine this possibility more fully, we have compared the hardness ratios (HRs) of stars with and without rotation periods, since HR is also correlated with accretion (accretors produce harder HRs; see §3.3.3). We find that the HRs of stars without rotation periods are marginally harder than those with rotation periods; a K-S test yields a probability of 1% that the distributions of HRs for the two groups are the same. Compared to the result in §3.3.3—where we found a highly statistically significant difference in HR for accretors vs. non-accretors—this suggests that, for the particular mix of stellar masses and accretion properties in the non- $P_{rot}$  sample, accretion is only weakly related to the lower average  $L_X$  of these stars. The significance of the effect is, nonetheless, comparable to the  $v \sin i$  effect described above.

Discerning whether, or to what extent, the lower average  $L_X$  of stars lacking rotation periods is due to accretion or slower rotation remains an open observational question. Unfortunately, the existing  $v \sin i$  study of Rhode, Herbst, & Mathieu (2001) did not have sufficiently high spectral resolution to place stringent lower limits on the rotation rates of these stars. It would thus be valuable to have high-resolution  $v \sin i$  measurements targeting stars with very low  $L_X$  and lacking  $P_{rot}$  in order to better constrain the slow extremes of rotation among stars that may represent the saturated and linear regimes ( $P_{rot} \gtrsim 20$  days) of the rotation/X-ray relationship.

Finally, we call attention to the fact that stars with rotation periods, despite evincing stable optical photometric variability with low levels of stochasticity (else their rotation periods would be difficult to measure), nonetheless show elevated levels of variability in X-rays (§3.1.2). This may suggest that the mechanism(s) responsible for X-ray variability are decoupled from the mechanism(s) often attributed to stochastic optical variability in PMS stars (i.e. accretion), as we now discuss.

## 4.2. Accretion

It is now generally accepted that most, if not all, PMS stars undergo a phase of active accretion whereby circumstellar material, perhaps channeled by stellar magnetic field lines, is deposited onto the stellar surface. Models of this accretion process (Calvet & Gullbring 1998; Gullbring et al. 1998; Valenti, Basri, & Johns 1993) have had some success in explaining the continuum excesses often observed in the UV among PMS stars as being due to the energetic shock that arises when accreted material impacts the stellar surface. Accretion is also typically implicated as the source of the stochastic, optical variability that is a defining characteristic of classical T Tauri stars (CTTS) (Herbst et al. 1994). It is appropriate to ask, therefore, whether X-rays from PMS stars may also have their origins, at least partly, in accretion.

We have already seen that X-ray variability is ubiquitous among the PMS stars in this study, despite the fact that the majority of these stars are weak-lined T Tauri stars (WTTS), as they do not show spectroscopic indicators of active accretion (§3.3.1). But perhaps accretion acts nonetheless to noticeably affect the X-ray emission of these stars. Indeed, we have seen that accretors and non-accretors do differ both in their X-ray luminosities (§3.3.2) and X-ray hardness (§3.3.3). Here we investigate these differences in greater detail.

We begin by reviewing the evidence, both from this study and from others in the literature, for a difference in the X-ray luminosities between accretors and non-accretors. We then present a simple model that explains these differences naturally in terms of enhanced X-ray *absorption* among stars with active accretion, due to the presence of magnetospheric accretion columns.

### 4.2.1. Differences in X-ray luminosities between accretors and non-accretors

Among PMS stars in a variety of star formation regions, there appears to be strong evidence for a difference in X-ray luminosity between accretors and non-accretors, in the sense that accretors tend to be underluminous in X-rays relative to non-accretors. A summary of the situation with a re-analysis of *ROSAT* data is presented in Flaccomio, Micela, & Sciortino (2003a) for the ONC, NGC 2264, and Chameleon I. Similar results are found by Neuhauser et al. (1995) in Taurus-Auriga.

However, the most recent observations in Orion present two different results. Flaccomio et al. (2003) find that that the difference in the median  $L_X$  between accreting and non-accreting stars is about one order of magnitude in the 0.25–2  $M_\odot$  range, in agreement with the earlier *ROSAT* findings. These authors use the EW of the Ca II lines, as reported by Hillenbrand et al. (1998), to distinguish accretors from non-accretors. Their study is based on a single exposure with *Chandra/HRC* (30' by 30') centered on  $\theta^1$  Ori C. Optical observations catalog 696 cluster members in the field, 342 of which are detected in the HRC image. Of the 696 possible members, a subset (304 stars) have  $\text{EW}(\text{Ca II}) < -1$  (108 X-ray detected, 58 undetected) or  $\text{EW}(\text{Ca II}) > 1$  (54 X-ray detected, 84 undetected). As the HRC instrument does not provide spectral information, the

authors assume a fixed plasma temperature for all sources and gas column density proportional to optical extinction in order to derive X-ray luminosities.

In contrast, Feigelson et al. (2002) find no difference in the distributions of CTTS and WTTS with respect to X-ray luminosity. Here, the distinction between CTTS and WTTS is made in terms of K-band excess, which is taken to indicate the presence of an accretion disk. Their study is based on the same *Chandra/ACIS* observations that we use in our own analysis. The ACIS image (17' by 17') is centered 22" west of  $\theta^1$ Ori C. In that region there are 529 optically detected stars, 525 of which are detected in the ACIS exposure.

The discrepancy between the findings of Flaccomio, Micela, & Sciortino (2003a) and Feigelson et al. (2002) can be resolved by noting that while infrared indicators signal the presence of a disk, this does not necessarily signal the presence of active accretion: the presence of a disk is presumably a prerequisite for accretion to occur, but not necessarily vice-versa. Indeed, using the same spectroscopic proxy for accretion as Flaccomio, Micela, & Sciortino (2003a), our analysis above (§3.3.2) confirms the findings of Flaccomio, Micela, & Sciortino (2003a) within the same ACIS observations used by Feigelson et al. (2002).

We thus take the finding of a difference in X-ray luminosity between accretors and non-accretors, as shown in Fig. 11, to be secure. In addition, we have found evidence for a difference between accretors and non-accretors in terms of X-ray hardness (Fig. 12). We now proceed to examine possible explanations for these differences.

#### 4.2.2. *Explanation: Enhanced X-ray emission or circumstellar absorption?*

PMS stars undergoing active accretion show systematically lower X-ray luminosities and harder X-ray hardness ratios (HR) than their non-accreting counterparts. This suggests that either: (a) the X-ray emission from accretors is intrinsically different in its spectral properties, namely, more concentrated to higher X-ray energies (i.e. harder); or (b) the X-ray emission from the accretors is intrinsically similar to that from non-accretors, but has been processed by circumstellar gas, preferentially attenuating X-rays at softer energies.

In the magnetospheric picture of accretion, CTTS are engaged in funnels of inflowing gas (Muzerolle, Calvet, & Hartmann 2001) with densities ranging from  $10^{12}$  to  $10^{14}$   $\text{cm}^{-3}$  (Calvet & Gullbring 1998). These funnels may be  $0.1 R_{\odot}$  thick, which implies that hydrogen column densities larger than  $10^{22}$   $\text{cm}^{-2}$  are possible. The exact amount of gas column will depend on the accretion rate and on the detailed geometry of the accretion flows but, as we show below, this amount of hydrogen column is potentially sufficient to both attenuate and harden the X-rays observed from CTTS.

To investigate this further, we first need to obtain the intrinsic (corrected for ISM absorption) X-ray characteristics of the *Chandra* sources. The X-ray luminosities and HRs that we have so

far used in our analysis have not been corrected for the attenuation and hardening caused by absorption due to interstellar gas. In some star formation regions, this is an important issue. For example, Neuhauser et al. (1995) have shown that in Taurus the reddening toward CTTS is significantly higher than toward WTTS, which could produce systematic differences in  $L_X$  and HR similar to what we have observed. In the Feigelson et al. (2002) data there is no evidence for a systematic difference in extinction between accretors and non-accretors; the extinction properties of both groups are the same to within 20%. Nonetheless, there may still be individual differences in extinction that could act to alter the medians in Figs. 11 and 12.

In order to correct for interstellar reddening we have performed the following analysis. We first calculate HR and  $L_X$  values for a grid of hydrogen column densities and plasma temperatures (Fig. 14). To generate these models, we used the Xspec code (Arnaud 1996), version 11.2, assuming a uniform plasma with  $0.3\times$  solar elemental abundances. As in Feigelson et al. (2002), continuum and line emission strengths were evaluated using the MEKAL code (Mewe 1991), and X-ray absorption was modeled using the cross sections of Morrison & McCammon (1983). For each star in the Feigelson et al. (2002) database, we take the HR and  $L_X$  values reported by them and extinctions ( $A_V$ ) from Hillenbrand (1997). We then use the relation  $N_H = 2 \times 10^{21} A_V$  to convert the observed extinctions into a measure of the hydrogen column density toward each star. From Fig. 14, we obtain the ratio between the observed luminosity and the luminosity corrected for reddening. For example, if a star is observed to have HR = 0.0 and  $A_V = 1.5$ , Fig. 14 tells us that the observed  $L_X = 0.6$  (arbitrary units) and that the intrinsic  $L_X = 0.9$  (obtained by moving in constant  $kT$  to  $A_V = 0$ ), implying that the X-ray luminosity has been extinguished by a factor of  $\sim 0.7$  and that the true HR is  $\sim -0.3$ . In this way we obtain corrected values of  $L_X$  and HR for each star. The results are shown in Figs. 15 and 16. The temperature obtained by this procedure should be regarded as an “effective” plasma temperature, as individual fits suggest that in some cases multiple plasmas, each with a different temperature, are necessary to reproduce the observations. The procedure also assumes that the plasma is in ionization equilibrium (Ardila et al. 2003).

After correcting for reddening, the differences in the histograms persist (Figs. 15a and 16a), although when plotted as functions of mass (Figs. 15b and 16b) the differences between the accretors and non-accretors become more subtle. It is therefore legitimate to ask whether the differences in the histograms are real, considering the dependence of  $L_X$  and HR on mass. For example, the presence of proportionately more non-accretors than accretors at higher masses could potentially explain the differences in the histograms. A two-way analysis of variance indicates that the  $L_X$  averages of accretors and non-accretors, after eliminating the effect of the mass, have a probability of  $1 \times 10^{-3}$  of being the same. For HR, the probability is  $1 \times 10^{-4}$ . In other words, there is a statistically significant difference between accretors and non-accretors, both in HR and in  $L_X$ , even after controlling for the mass dependence. Interestingly, HR appears to increase (albeit weakly) with mass—the analysis of variance indicates that the probability of all the means in the mass bins being the same is  $10^{-3}$ —perhaps implying that more massive stars have hotter chromospheres. This is not due to the fact that higher mass stars have higher  $L_X$ ; HR is scale-independent, so

overall increases in  $L_X$  do not affect it.

Differences in HR values between CTTS and WTTS have been reported in the literature for Taurus, Lupus, Chameleon, Sco-Cen, and the TW Hya association (Neuhauser, Sterzik, & Schmitt 1994; Krautter et al. 1994; Neuhauser et al. 1995; Kastner et al. 2002). All these are based on *ROSAT* data, for which two different hardness ratios are traditionally defined in the literature:  $HR1 = (Z_{h1} + Z_{h2} - Z_s)/(Z_{h1} + Z_{h2} + Z_s)$ —where  $Z_{h1}$  is the count rate from 0.5 to 0.9 keV,  $Z_{h2}$  is from 0.9 to 2 keV, and  $Z_s$  is from 0.1 to 0.4 keV—and  $HR2 = (Z_{h1} - Z_{h2})/(Z_{h1} + Z_{h2})$ . Note that the two “hard” *ROSAT* bands are equivalent to the “soft” *Chandra* band so the results from *Chandra* and *ROSAT* are not directly comparable. In the *ROSAT* observations, and for these star formation regions, the WTTS are as a group significantly softer than the CTTS in the HR1 ratio, while the two populations have similar HR2 ratios. Our analysis shows that the difference reappears in the higher energy *Chandra* HR ratio, which samples energies up to 8 keV. Neuhauser et al. (1995), finding no difference in emission temperatures between CTTS and WTTS in Taurus, and considering different star-forming regions with different extinction characteristics, argue that this difference in HR is due to absorption in the circumstellar environs of the CTTS (circumstellar disks, remnant nebulae and envelopes, outflows, etc.).

For the observations presented here, the differences in  $L_X$  and HR between accretors and non-accretors are consistent with a picture in which CTTS have intrinsically similar X-ray emission properties as WTTS, with X-rays from the former being extinguished by circumstellar gas in amounts consistent with that predicted for magnetospheric accretion columns. The median HR (corrected for absorption) of the non-accretors in our sample is  $-0.40$  with  $\sigma = 0.3$ . For the accretors, the value is  $-0.23$  with  $\sigma = 0.3$ . Assuming that the difference is due to gas absorption, we can use Fig. 14 to obtain the gas column density. If the mean HR of the non-accretors in our sample ( $-0.40$ ) represents the intrinsic HR of a T Tauri star, this implies (following the  $A_V = 0.0$  curve) a plasma temperature of  $kT \sim 1.7$  keV. The curves are marked in dust extinction magnitudes, but in this exercise we are using them to correct for gas absorption only. If we follow the line of constant  $kT$  to higher hardness ratios, we reach  $HR \approx -0.2$  at  $A_V \approx 1.0$ , which implies  $2 \times 10^{21} \text{ cm}^{-2}$ . In this case, the ratio in  $L_X$  between accretors and non-accretors would be  $\sim 0.7$ . Given the width of the HR histograms, column densities as large as  $10^{22} \text{ cm}^{-2}$  of gas may be necessary. These produce ratios in  $L_X$  as large as 0.8 dex, which is consistent with Fig. 15 and with the results of Flaccomio, Micela, & Sciortino (2003a).

On the other hand, Kastner et al. (2002) argue, on the basis of *Chandra* X-ray spectroscopy, that the X-ray emission from TW Hya is due to the accretion shock at the base of the accretion column, and not simply to attenuated WTTS emission. The differential emission measure is quite unlike that of other active evolved stars (even though it is not clear what one should expect for a PMS star). TW Hya is a 10 Myr old,  $0.7 M_\odot$  PMS star with  $L_X \sim 10^{30} \text{ erg/sec}$ , and so it has a very average position in our  $L_X$  vs. mass diagram. This star poses a puzzle for the arguments presented here in favor of a common origin for X-ray emission in CTTS and WTTS. Its accretion rate has been reported as being  $5\text{--}100 \text{ } 10^{-10} M_\odot/\text{yr}$  (Muzerolle, Calvet, & Hartmann 2001; Alencar

& Batalha 2001), and if the lower limit is right, one would expect essentially no gas attenuation. In addition, coronal activity decreases with age, and so perhaps the observations of TW Hya are not applicable to younger samples. Certainly, X-ray spectroscopic observations of young WTTS and CTTS are needed before this issue can be fully resolved.

## 5. Summary and Conclusions

We have re-analyzed all archival *Chandra/ACIS* observations of pre-main-sequence (PMS) stars with optically determined rotation periods in the Orion Nebula Cluster (ONC). Our aim is to investigate the relationship between X-rays and the physical mechanisms most likely related to their production in PMS stars: rotation and accretion. Our analysis procedures include filtering of flare events in the X-ray data in an attempt to determine X-ray luminosities that are free of the stochasticity introduced by such events.

The primary findings of this study are as follows:

1. Stars with optically determined rotation periods are more X-ray luminous, and are more likely to be X-ray variable, than are stars without optical rotation periods. We show that the bias to high  $L_X$  is not due to a magnitude bias in optical rotation-period studies of the ONC; rather, it is due to the diminishingly small amplitude of optical variability among stars with smaller  $L_X$ , precluding detection of their rotation periods.
2. Stars with optically determined rotation periods have a mean  $L_X/L_{bol}$  near, but lower than, the “saturation” value of  $\sim 10^{-3}$ , implying that these stars are in the saturated or super-saturated regimes of the X-ray/rotation relationship, consistent with their Rossby numbers. There is a marginally significant ( $\sim 3\sigma$ ) correlation between  $L_X/L_{bol}$  and  $P_{rot}$ , with the more rapidly rotating stars showing lower  $L_X/L_{bol}$ , as is seen among super-saturated stars on the main sequence.
3. Compared to these stars, stars *without* rotation periods show a larger range of  $L_X/L_{bol}$ —comparable, in fact, to that found among main sequence stars. We consider the possibility that, among these, some stars may lie at the beginnings of the “linear” regime of the X-ray/rotation relationship. Using  $v \sin i$  data from the literature we find that, among these stars lacking known rotation periods, slower rotators do indeed show lower X-ray luminosities than do rapid rotators. This relationship is not one-to-one, however. It is also possible that the lower  $L_X$  among stars lacking rotation periods is instead due to the higher incidence of active accretion among these stars, a possibility for which we also find weak evidence. The statistical significance of these two effects— $v \sin i$  and accretion—are comparable. Measurements of  $v \sin i$  sensitive to very slow rotators ( $\lesssim 5$  km/s) would be of great value in furthering our understanding of X-ray production at the slow extremes of PMS rotation. PMS stars in the linear regime should have  $P_{rot} \gtrsim 100$  days, assuming a typical convective turnover timescale

of  $\tau_c \sim 800$  days. Such long rotation periods have yet to be observed among PMS stars.

4. Stars in the ONC with spectroscopic signatures of active accretion show significantly harder X-ray spectra and lower X-ray luminosities than their non-accreting counterparts. These observations can be explained quantitatively by a model in which accretors and non-accretors have intrinsically similar X-ray emission properties, with the differences in  $L_X$  and hardness ratio being due to absorption of soft X-rays by magnetospheric accretion columns.

Taken together, these findings hint that there in fact exists a rotation-activity relationship among PMS stars in the ONC, and suggest that rotation—not accretion—is the primary driver of X-ray emission in low-mass ( $M \lesssim 3 M_\odot$ ) PMS stars at 1 Myr. Indeed, our finding that stars with rotation periods show elevated levels of X-ray variability, despite showing little stochastic variability in the optical, further implies that X-ray variability has its origins in processes that are more or less independent of the processes responsible for stochastic variability in the optical (i.e. accretion).

Finally, our findings raise questions about the true physical meaning of “saturation” in PMS stars. It is intriguing that stars with optically determined rotation periods all appear to lie in the super-saturated regime yet show diminishingly small amplitudes of optical variability at low  $L_X$ . It is possible that spots on the surfaces of these stars become non-existent below a certain  $L_X$  threshold. On the other hand, we speculate that the low amplitude of optical variability may be due to magnetic topologies in which the stellar surface is indeed largely covered by spots, but spots that are more-or-less randomly distributed over the stellar surface, thereby producing only very small photometric signals in the optical. More organized magnetic topologies may be present in stars with higher  $L_X$ , such that larger spots asymmetrically distributed on the stellar surface are possible. In this picture, these latter stars might be those whose global fields have become sufficiently organized and deeply rooted so as to begin effecting magnetic braking of the stellar rotation, a picture similar to that recently put forward by Barnes (2003a,b).

We acknowledge funding under Chandra Award Number AR2-3001X issued by the Chandra X-Ray Observatory Center, which is operated by the Smithsonian Astrophysical Observatory on behalf of NASA under contract NAS8-390073. We also gratefully acknowledge the useful comments of the anonymous referee.

## REFERENCES

- Alencar, S. H. P. & Batalha, C., 2001, ASP Conf. Ser. 244: Young Stars Near Earth: Progress and Prospects, pg.141
- Ardila, D. R., et al. 2003, in “Open Issues in Local Star Formation”, in press
- Arnaud, K. A. 1996, ASP Conf. Ser. 101: Astronomical Data Analysis Software and Systems V, 17

- Barnes, S. A. 2003b, *ApJ*, 586, L145
- Barnes, S. A. 2003a, *ApJ*, 586, 464
- Bouvier, J., Forestini, M., & Allain, S. 1997, *A&A*, 326, 1023
- Caillault, J.-P. 1996, *ASP Conf. Ser.* 109: Cool Stars, Stellar Systems, and the Sun, 9, 325
- Calvet, N., & Gullbring, E. 1998, *ApJ*, 509, 802
- Feigelson, E., & Montmerle, T. 1999, *ARA&A*, 37, 363
- Feigelson, E. D., Gaffney, J. A., Garmire, G., Hillenbrand, L. A., Townsley, L. 2003, *ApJ*, 584, 911
- Feigelson, E. D., Broos, P., Gaffney, J. A., Garmire, G., Hillenbrand, L. A., Pravdo, S. H., Townsley, L., & Tsuboi, Y. 2002, *ApJ*, 574, 258
- Flaccomio, E., Micela, G., & Sciortino, S. 2003b, *A&A*, 402, 277
- Flaccomio, E., Micela, G., & Sciortino, S. 2003a, *A&A*, 397, 611
- Flaccomio, E., Damiani, F., Micela, G., Sciortino, S., Harnden, F. R., Murray, S. S., & Wolk, S. J. 2003, *ApJ*, 582, 398
- Flaccomio, E. 2002, Ph.D. Thesis, Università degli Studi di Palermo
- Gullbring, E., Hartmann, L., Briceno, C., & Calvet, N. 1998, *ApJ*, 492, 323
- Herbst, W., Bailer-Jones, C. A. L., Mundt, R., Meisenheimer, K., & Wackermann, R. 2002, *A&A*, 396, 513
- Herbst, W., Herbst, D. K., Grossman, E. J., & Weinstein, D. 1994, *AJ*, 108, 1906
- Hillenbrand, L. A. 1997, *AJ*, 113, 1733
- Hillenbrand, L. A., Strom, S. E., Calvet, N., Merrill, K. M., Gatley, I., Makidon, R. B., Meyer, M. R., & Skrutskie, M. F. 1998, *AJ*, 116, 1816
- James, D. J., Jardine, M. M., Jeffries, R. D., Randich, S., Collier Cameron, A., & Ferreira, M. 2000, *MNRAS*, 318, 1217
- Jeffries, R.D. 1999, *ASP Conf. Ser.* 158: Solar and Stellar Activity: Similarities and Differences, 75
- Kastner, J. H., Crigger, L., Rich, M., & Weintraub, D. A. 2002, *ApJ*, 585, 878
- Kim, Y. & Demarque, P. 1996, *ApJ*, 457, 340
- Krautter, J., Alcalá, J. M., Wichmann, R., Neuhauser, R., & Schmitt, J. H. M. M. 1994, *Revista Mexicana de Astronomía y Astrofísica*, 29, 41

- Krishnamurthi, A., Pinsonneault, M. H., Barnes, S., & Sofia, S. 1997, *ApJ*, 480, 303
- Mewe, R. 1991, *ARA&A*, 3, 127
- Morrison, R., & McCammon, D. 1983, *ApJ*, 270, 119
- Muzerolle, J., Calvet, N., & Hartmann, L. 2001, *ApJ*, 550, 944
- Neuhauser, R., Sterzik, M. F., Schmitt, J. H. M. M., Wichmann, R., & Krautter, J. 1995, *A&A*, 297, 391
- Neuhauser, R., Sterzik, M. F., & Schmitt, J. H. M. M. 1994, in *ASP Conf. Ser. 64: Cool Stars, Stellar Systems, and the Sun*, 113
- Pallavicini, R., Golub, L., Rosner, R., Vaiana, G. S., Ayres, T., & Linsky, J. L. 1981, *ApJ*, 248, 279
- Pizzolato, N., Maggio, A., Micela, G., Sciortino, S., & Ventura, P. 2003, *A&A*, 397, 147
- Randich, S. 2000, *ASP Conf. Ser. 198: Stellar Clusters and Associations: Convection, Rotation, and Dynamos*, 401
- Randich, S. 1997, *Memorie della Societa Astronomica Italiana*, 68, 971
- Rhode, K. L., Herbst, W., & Mathieu, R. D. 2001, *AJ*, 122, 3258
- Stassun, K. G., Mathieu, R. D., Mazeh, T., & Vrba, F. J. 1999, *AJ*, 117, 2941
- Stelzer, B. & Neuhäuser, R. 2001, *A&A*, 377, 538
- Tsujiimoto, M., Koyama, K., Tsuboi, Y., Goto, M., & Kobayashi, N. 2002, *ApJ*, 566, 974
- Valenti, J. A., Basri, G., & Johns, C. M. 1993, *AJ*, 106, 2024
- Ventura, P., Zeppieri, A., Mazzitelli, I., & D'Antona, F. 1998, *A&A*, 331, 1011

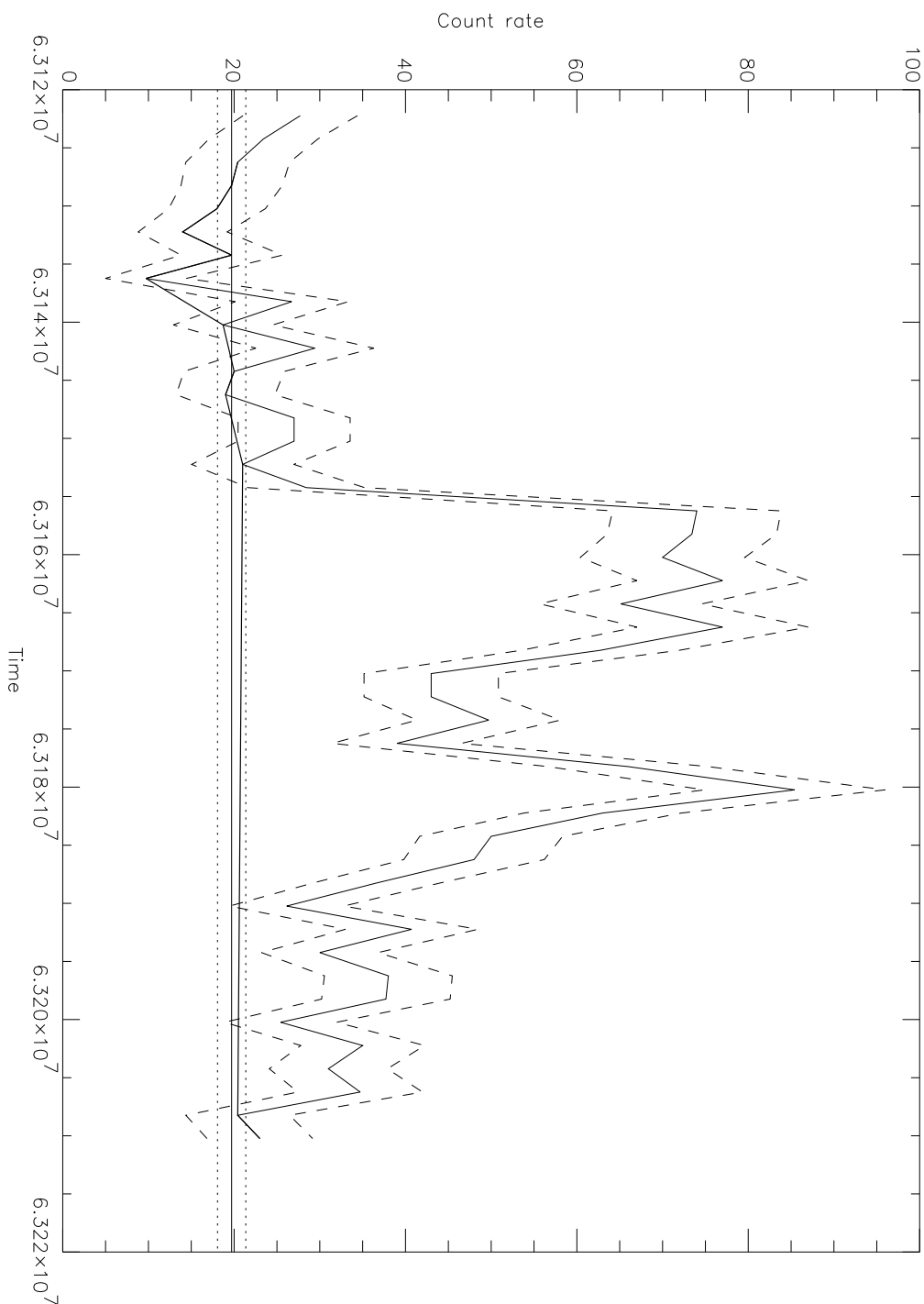


Fig. 1.— Example of light curve filtering for flare events for a source in the observation of Tsujimoto. The thin solid line represents the observed light curve, and dashed lines represent  $1\sigma$  errors based on simple counting statistics. The thick solid line represents the light curve after flare filtering. The horizontal solid and dotted lines indicate the quiescent count rate determined from the filtering procedure (solid line) and  $1\sigma$  errors (dotted).

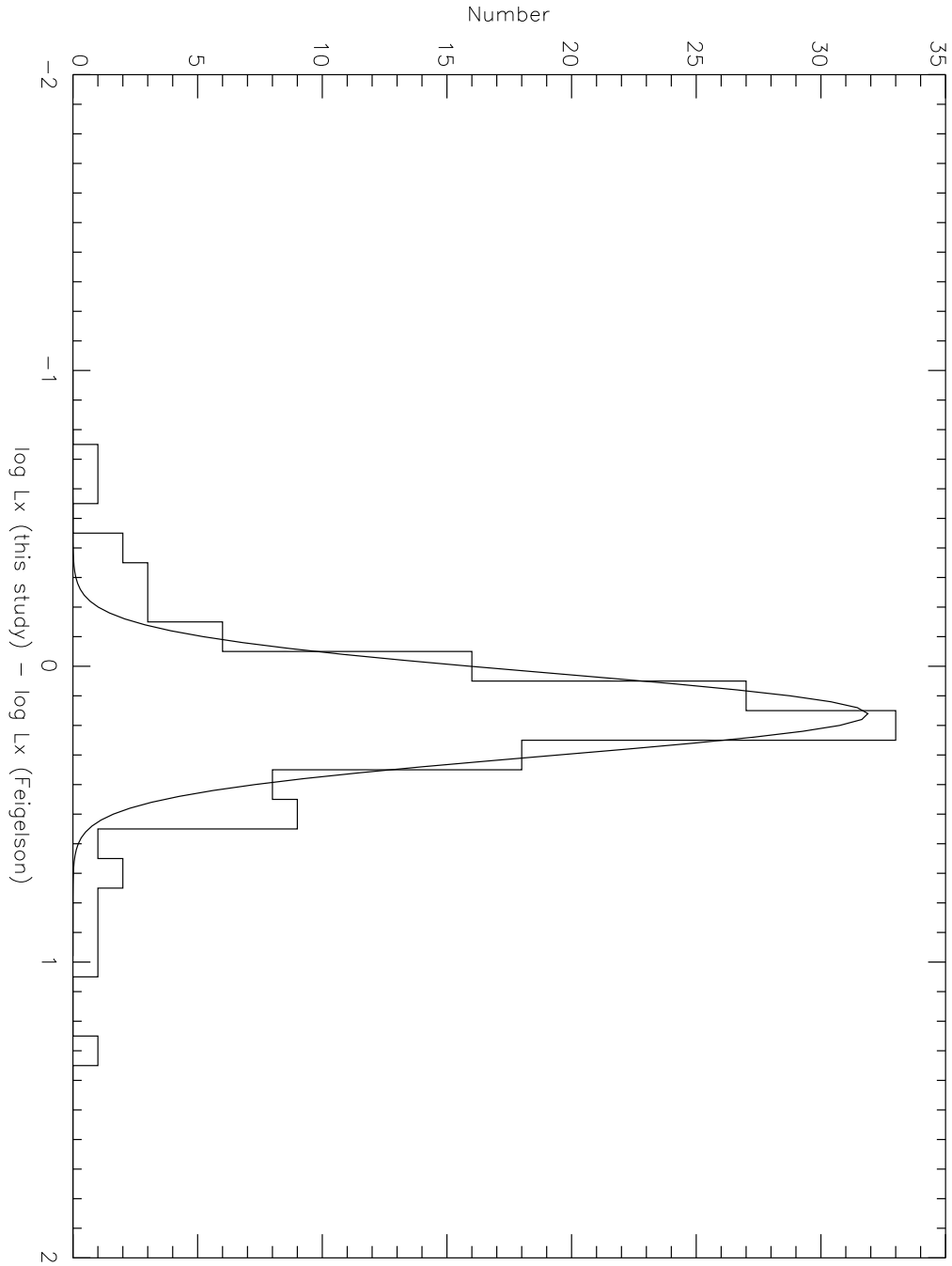


Fig. 2.— Differences between the  $L_X$  values measured by us and those reported by Feigelson et al. (2002) (histogram). The gaussian fit shown has  $\sigma = 0.14$  dex and an offset of 0.15 dex. Approximately 0.04 dex of this offset is due to the different distances assumed to the ONC by us (470 pc) and by Feigelson et al. (2002) (450 pc).

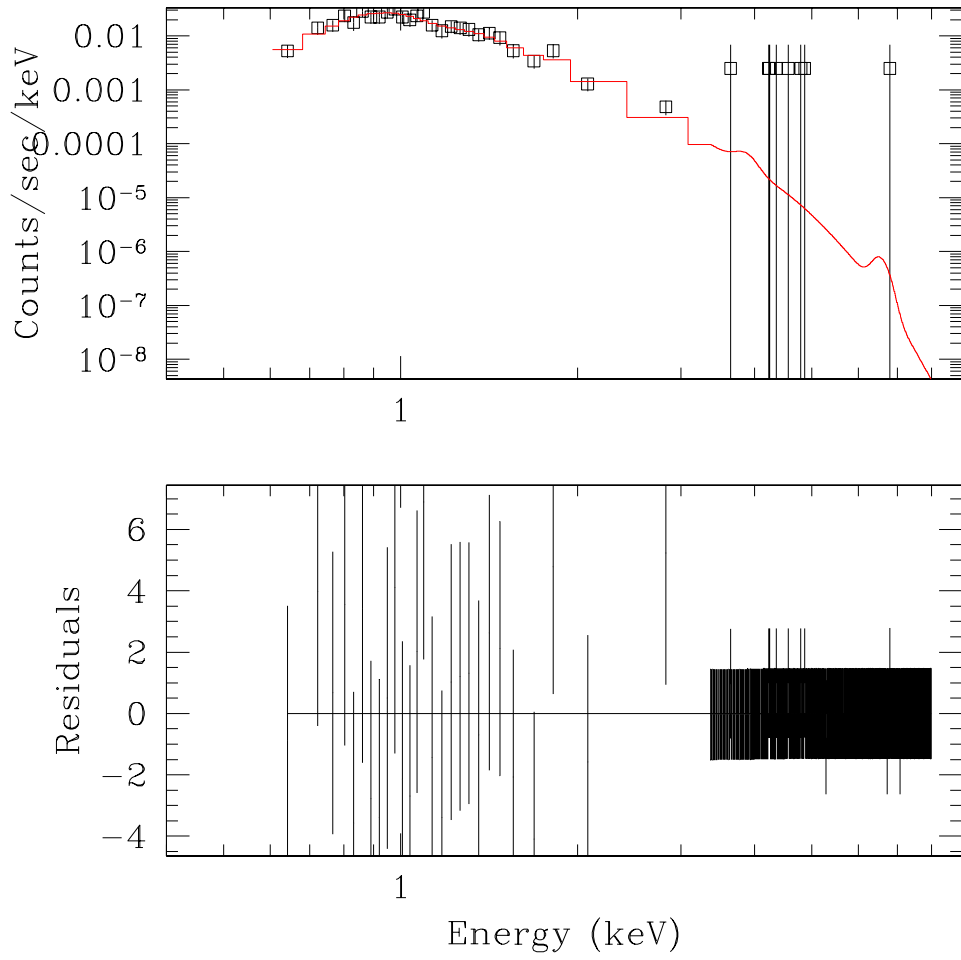


Fig. 3.— Results of SHERPA model fit to the *Chandra* spectrum of star 116 from the first Garmire exposure.

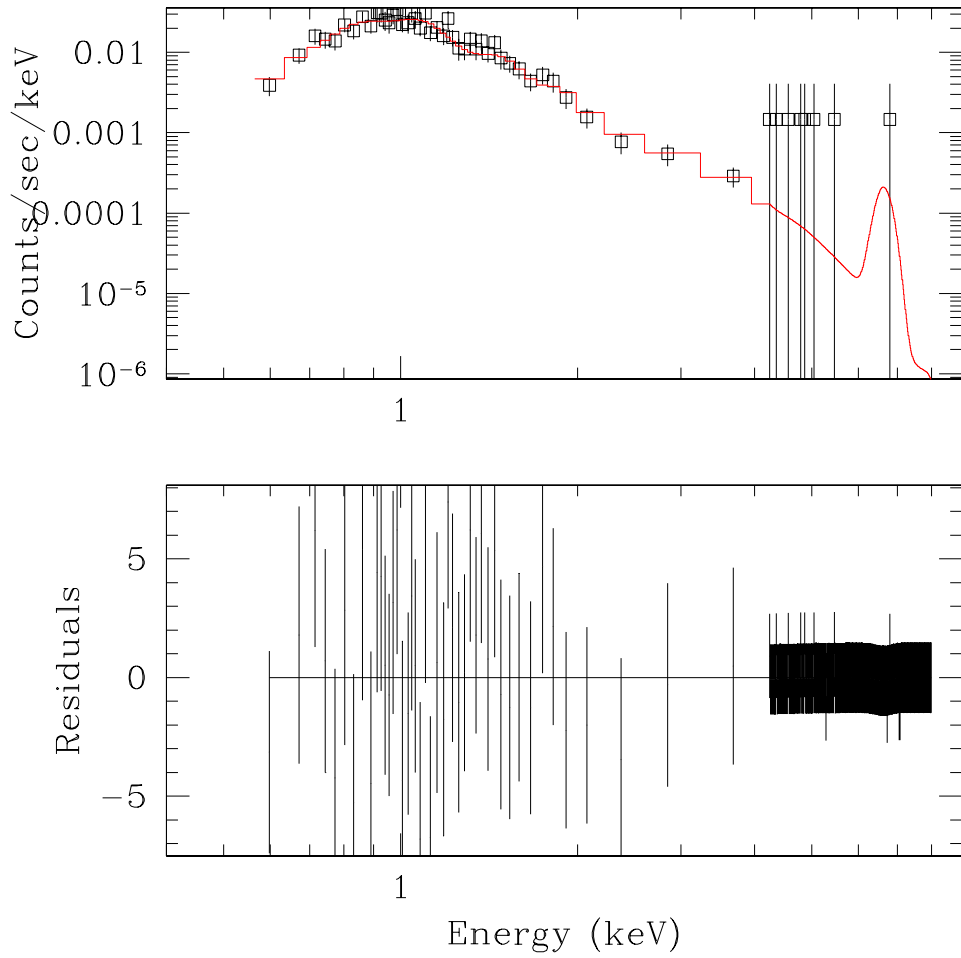


Fig. 4.— Results of SHERPA model fit to the *Chandra* spectrum of star 116 from the first Garmire exposure using pre-filtered data.

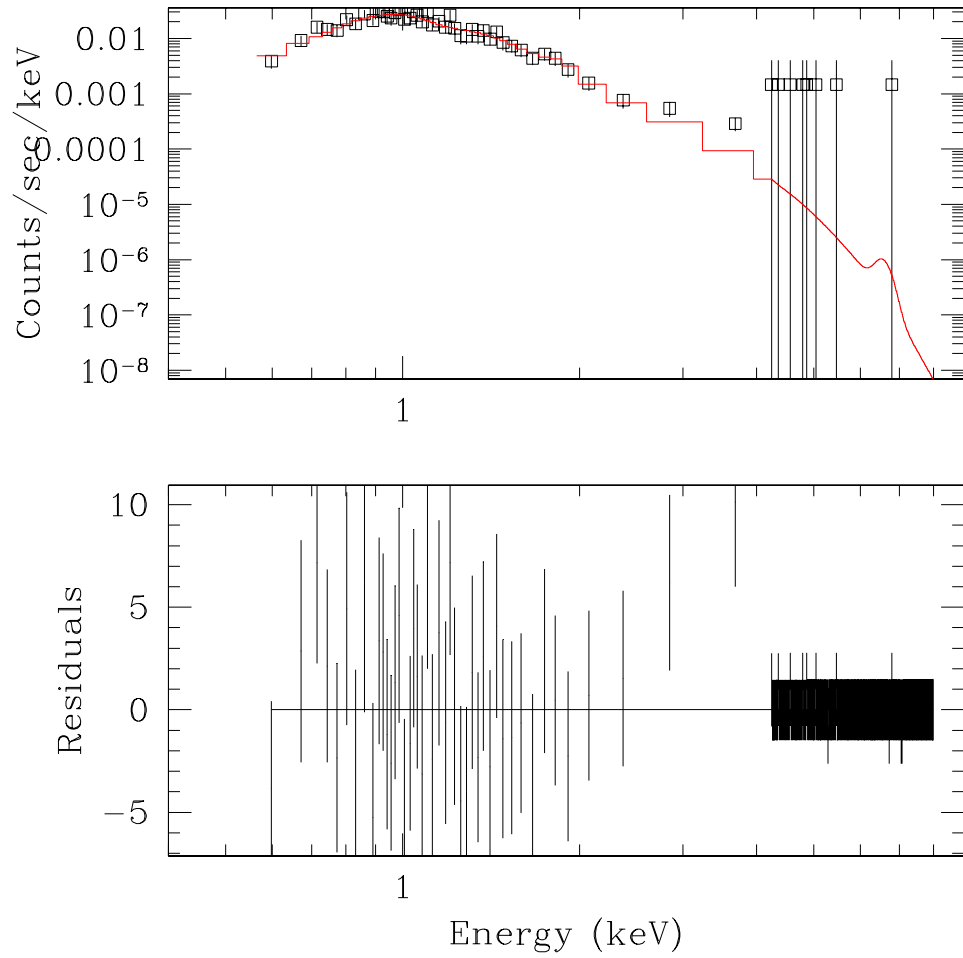


Fig. 5.— Results of SHERPA model fit to the *Chandra* spectrum of star 116 from the first Garmire exposure using pre-filtered data and a single-component thermal plasma model.

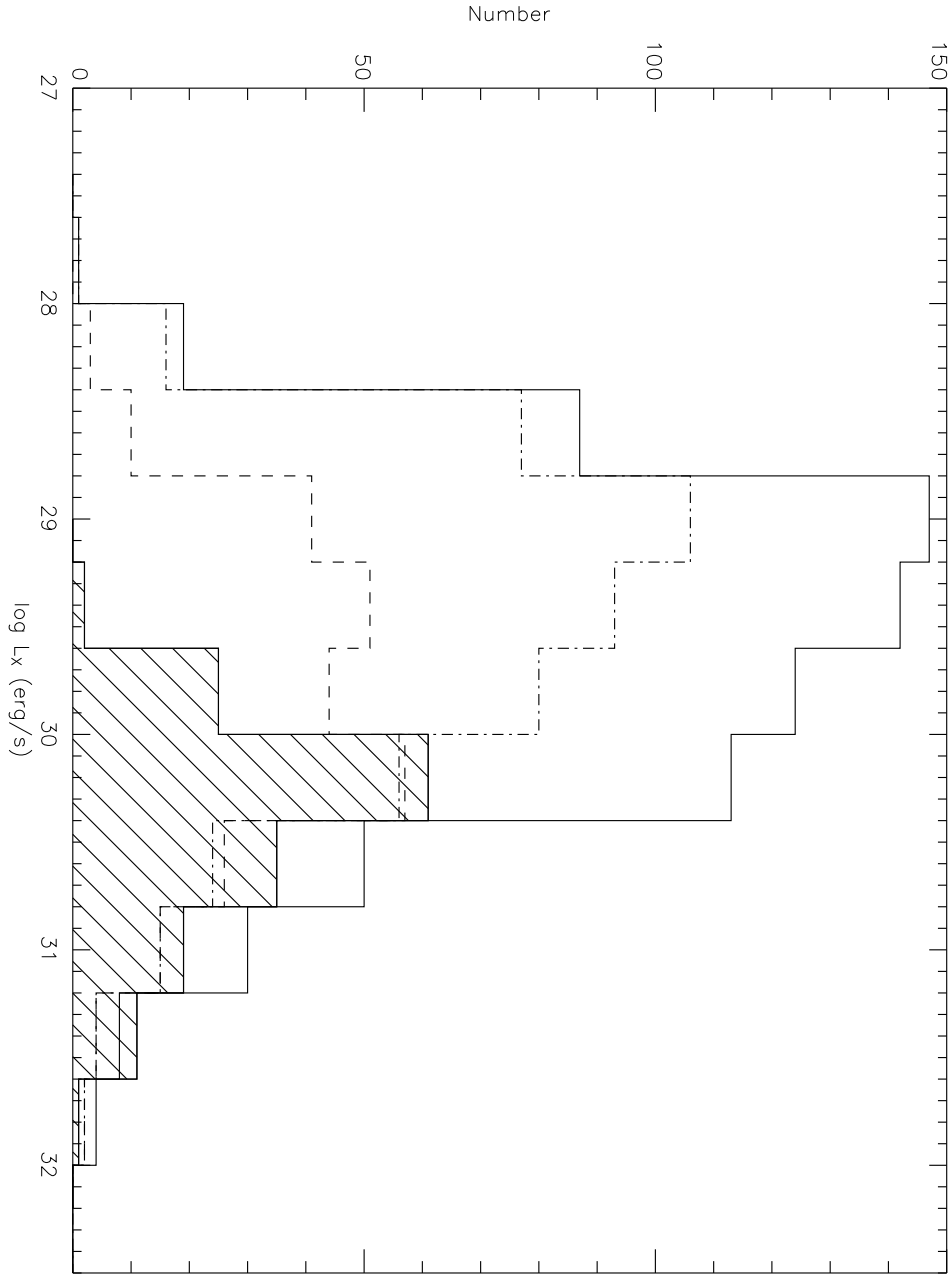


Fig. 6.— Distribution of  $\log L_X$  for all ONC stars with optically determined rotation periods detected by Feigelson et al. (2002) (dashed) and the distribution for those stars with high signal-to-noise detected in this study (hatched). For comparison, the solid histogram shows the distribution for all ONC stars detected by Feigelson et al. (2002) having optical magnitudes bright enough ( $I \lesssim 17$ ) to have been included in the optical rotation-period surveys of the ONC (Stassun et al. 1999; Herbst et al. 2002). The distribution for stars lacking rotation period measurements are indicated by the dot-dashed histogram. Stars with optically determined rotation periods are systematically biased to higher  $L_X$  as compared to the underlying population.

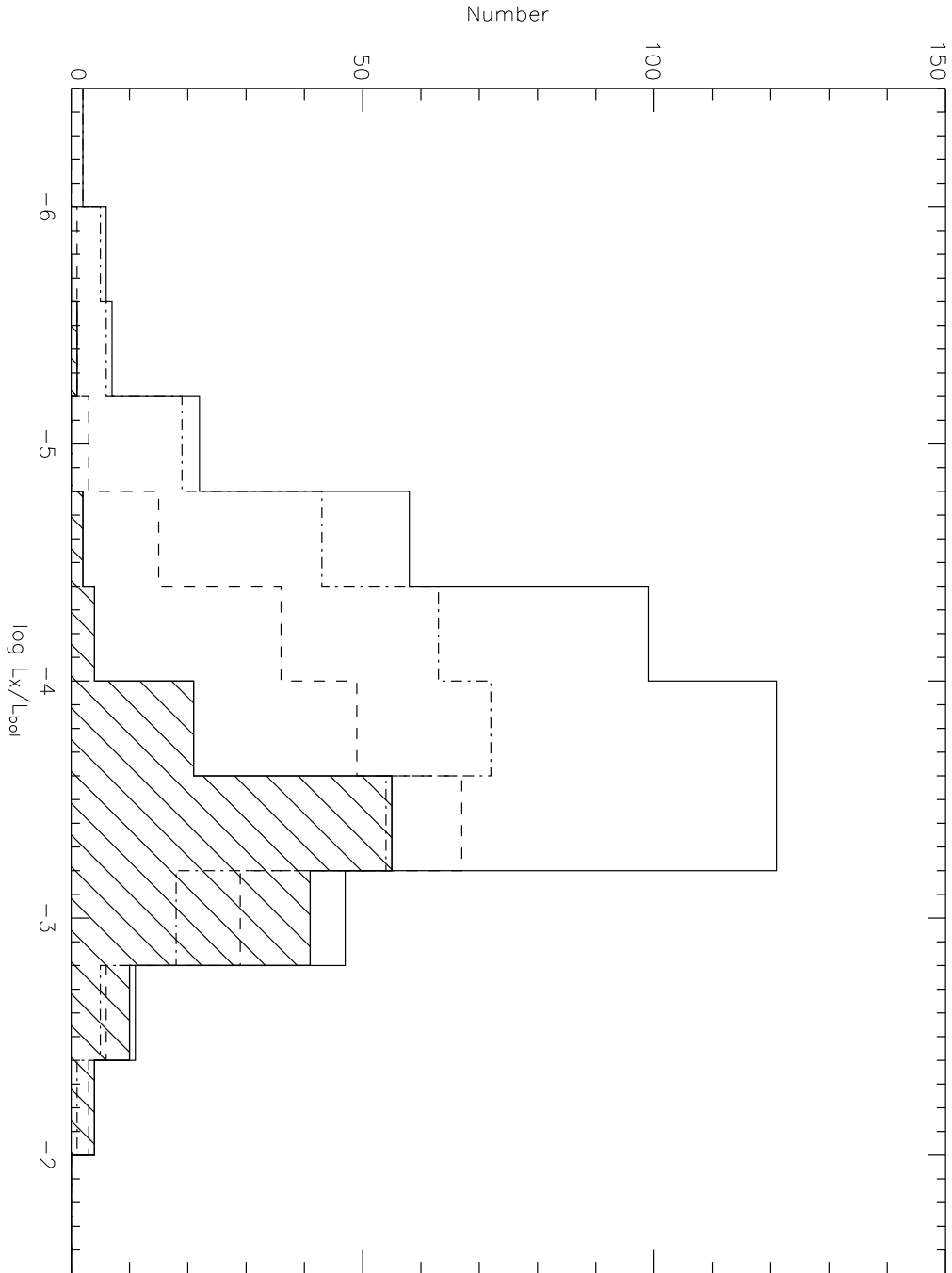


Fig. 7.— Same as Fig. 6, except showing  $L_X/L_{bol}$  instead of  $L_X$ . The bias for stars with rotation periods toward higher  $L_X$  is evident in  $L_X/L_{bol}$  also.

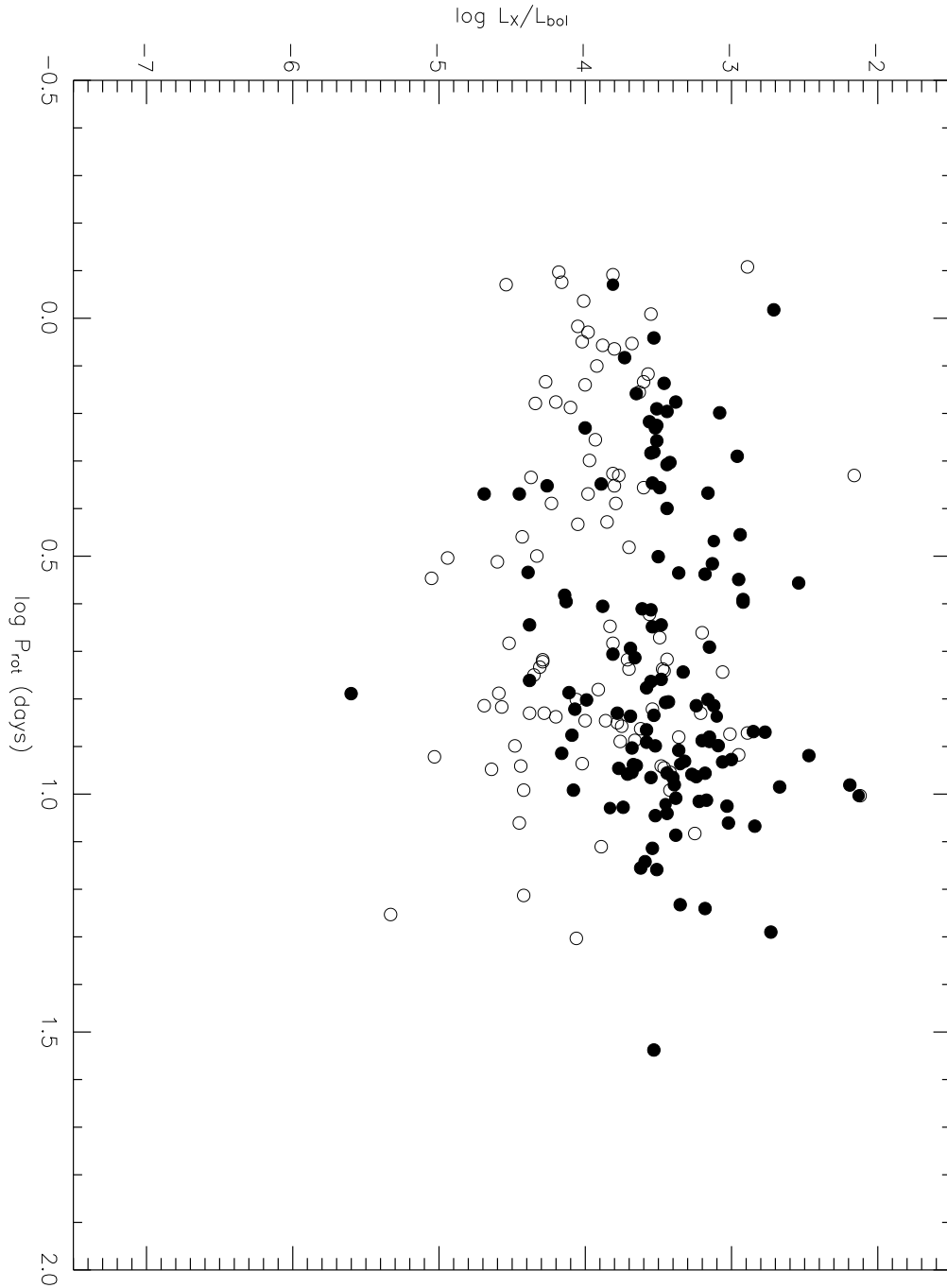


Fig. 8.— The X-ray/rotation relationship for PMS stars in the ONC with known rotation periods. Filled circles represent stars detected in this study, open circles represent additional stars from the study of Feigelson et al. (2002).

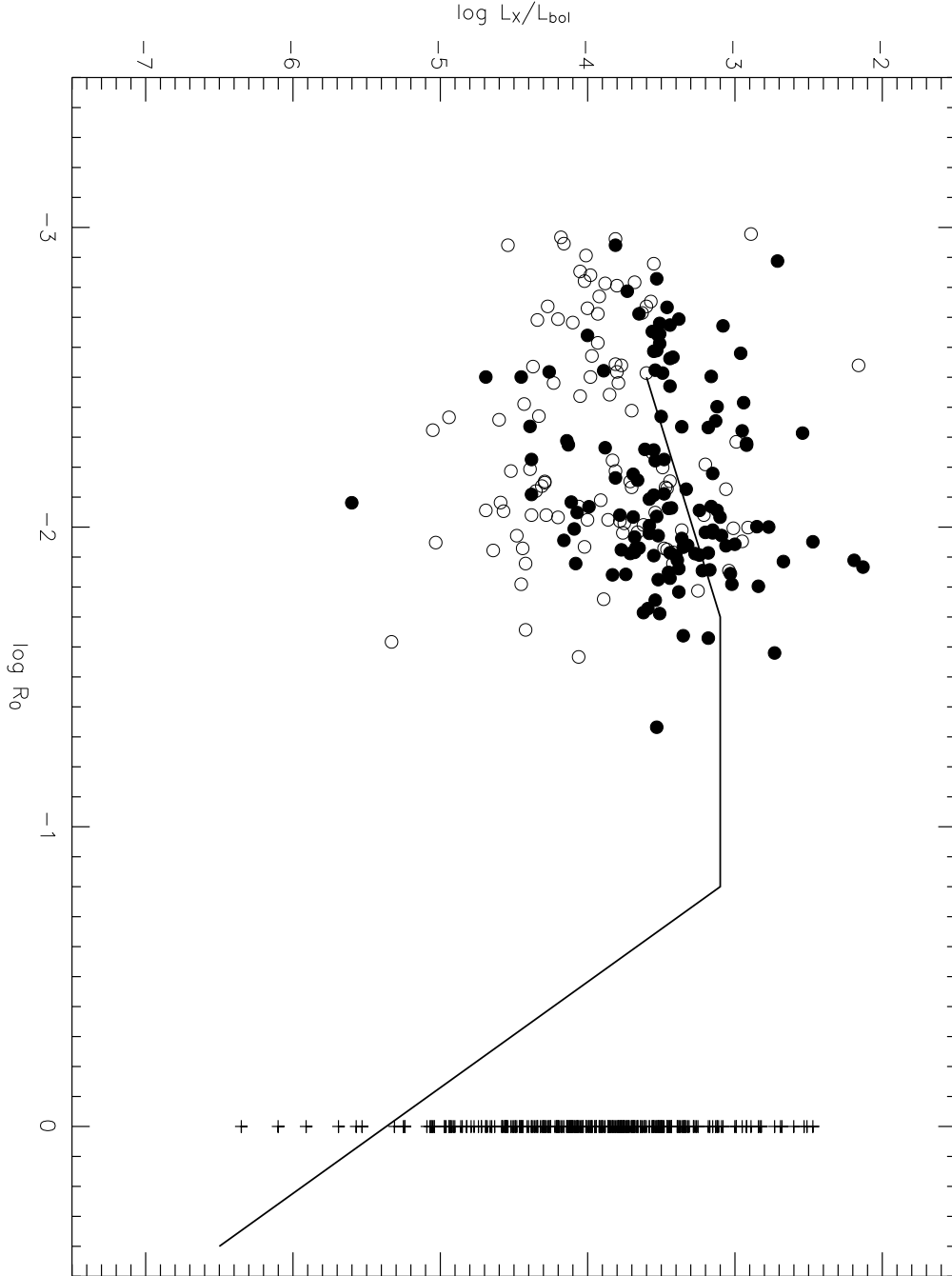


Fig. 9.— The X-ray/rotation relationship for PMS stars in the ONC with respect to Rossby number instead of  $P_{rot}$ . Point symbols are as in Fig. 8. The main sequence relationship is indicated by the solid line for comparison. Also shown (crosses) is the remainder of the sample included in the study of Feigelson et al. (2002) with  $M < 3 M_{\odot}$  (plotted arbitrarily at  $\log R_0 = 0$ ).

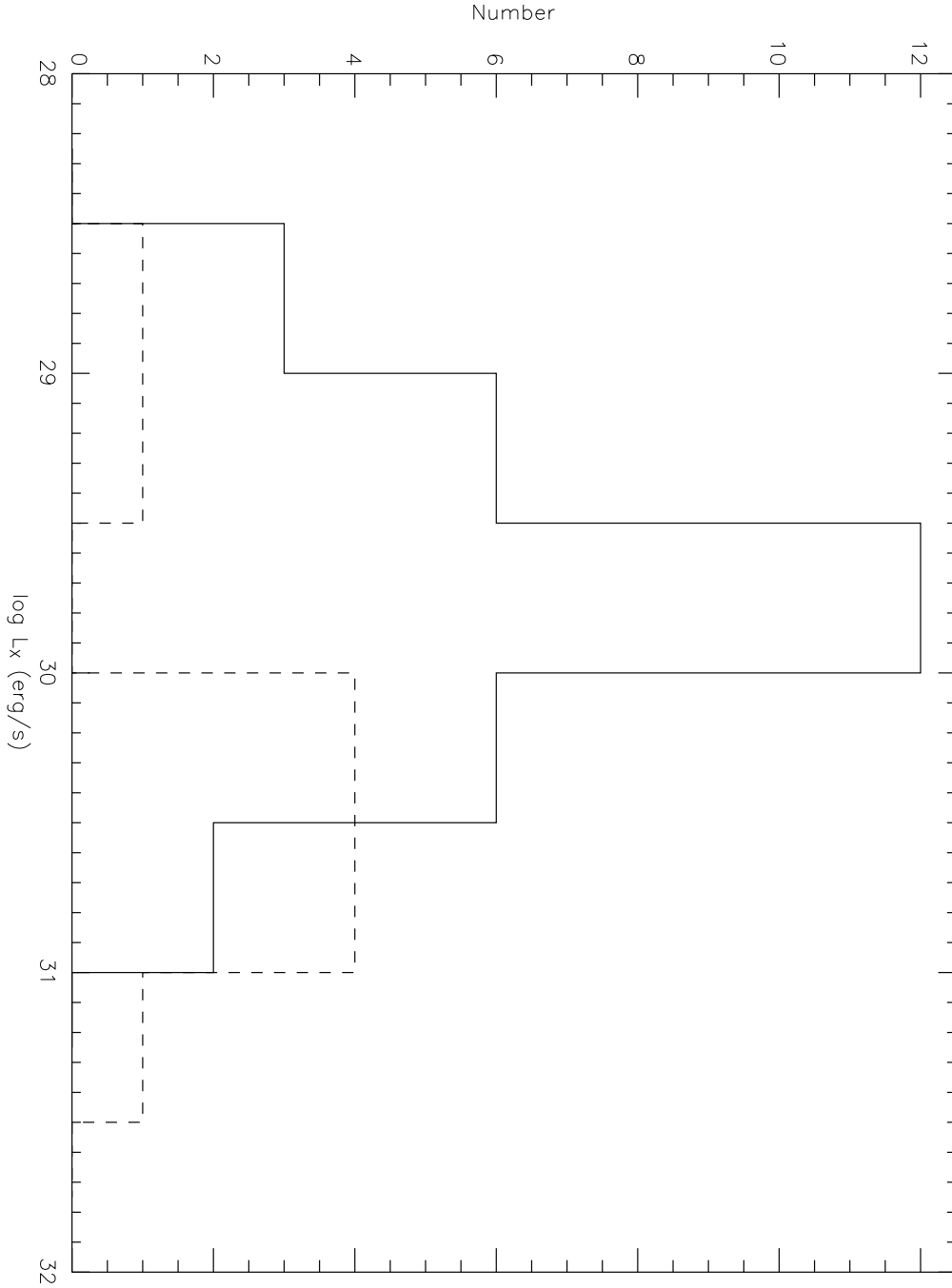


Fig. 10.— Distribution of  $\log L_X$  for stars lacking  $P_{\text{rot}}$  but with  $v \sin i$  measurements from Rhode, Herbst, & Mathieu (2001). The solid histogram represents slow rotators, defined as stars with  $v \sin i$  upper limits, whereas the dashed histogram represents rapid rotators, defined as stars with broadened spectral lines. Rhode, Herbst, & Mathieu (2001) report an instrumental resolution of  $\approx 14$  km/s.

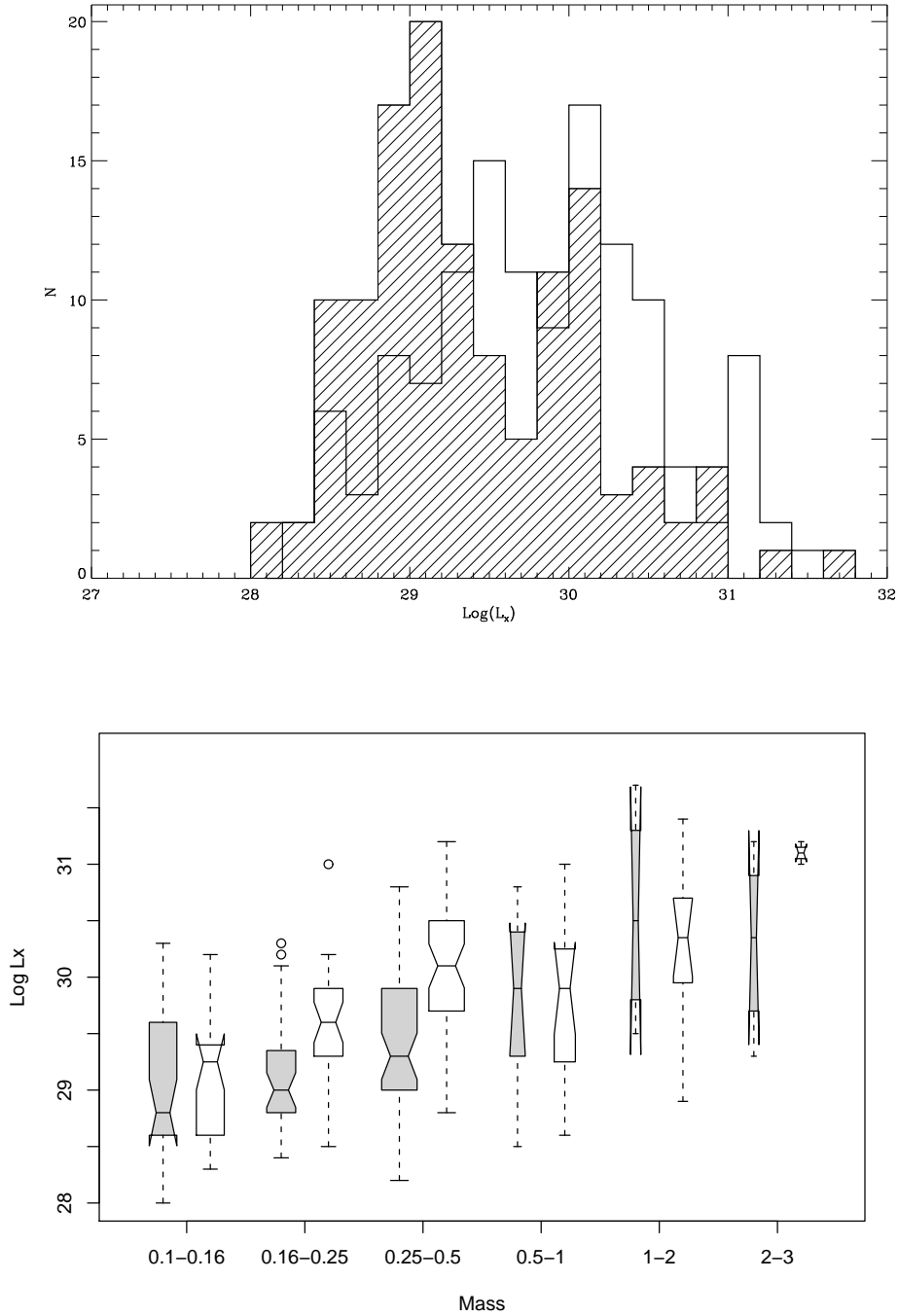


Fig. 11.— (Top) Distribution of X-ray luminosities for the Feigelson et al. (2002) data. The hatched (clear) histogram is for stars with  $\text{EW}(\text{Ca II}) < -1 \text{ \AA}$  ( $\text{EW}(\text{Ca II}) > 1 \text{ \AA}$ ). (Bottom) Box plots for X-ray luminosities, binned as a function of mass. The gray (clear) boxes correspond to accretors (non-accretors). The width of each box is proportional to the square root of observations in each bin. The scale of the abscissa is arbitrary. For the accretors, there are 29,32,48,9,4, and 4 stars in each increasing mass bin. For the non-accretors there are 26,28,42,15,12, and 4 stars.

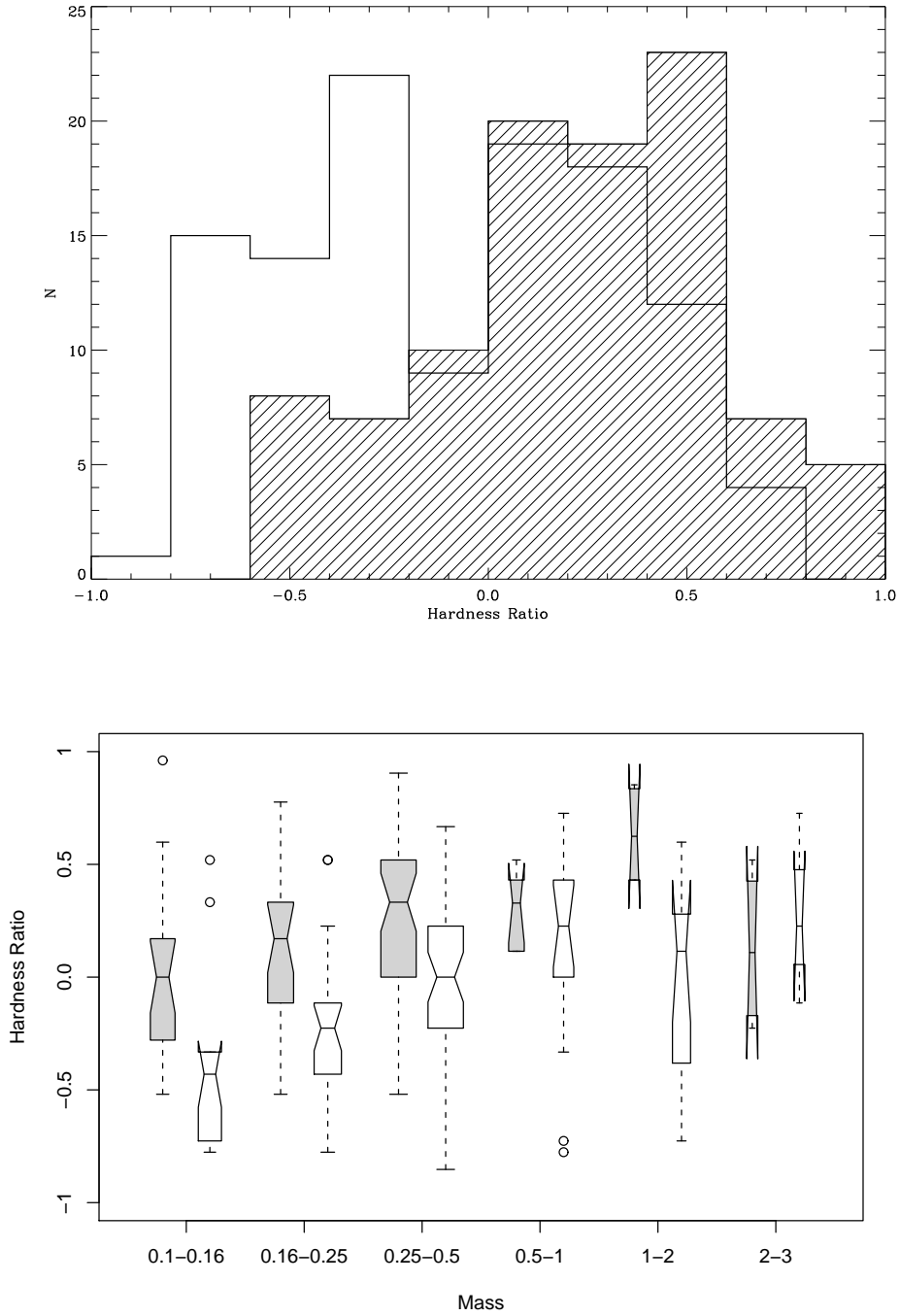


Fig. 12.— (Top) Distribution of HR for Feigelson et al. (2002) data. The hatched (clear) histogram is for stars with  $EW(\text{Ca II}) < -1 \text{ \AA}$  ( $EW(\text{Ca II}) > 1 \text{ \AA}$ ). (Bottom) Box plots for HR as a function of mass. As before, gray (clear) boxes correspond to accretors (non-accretors).

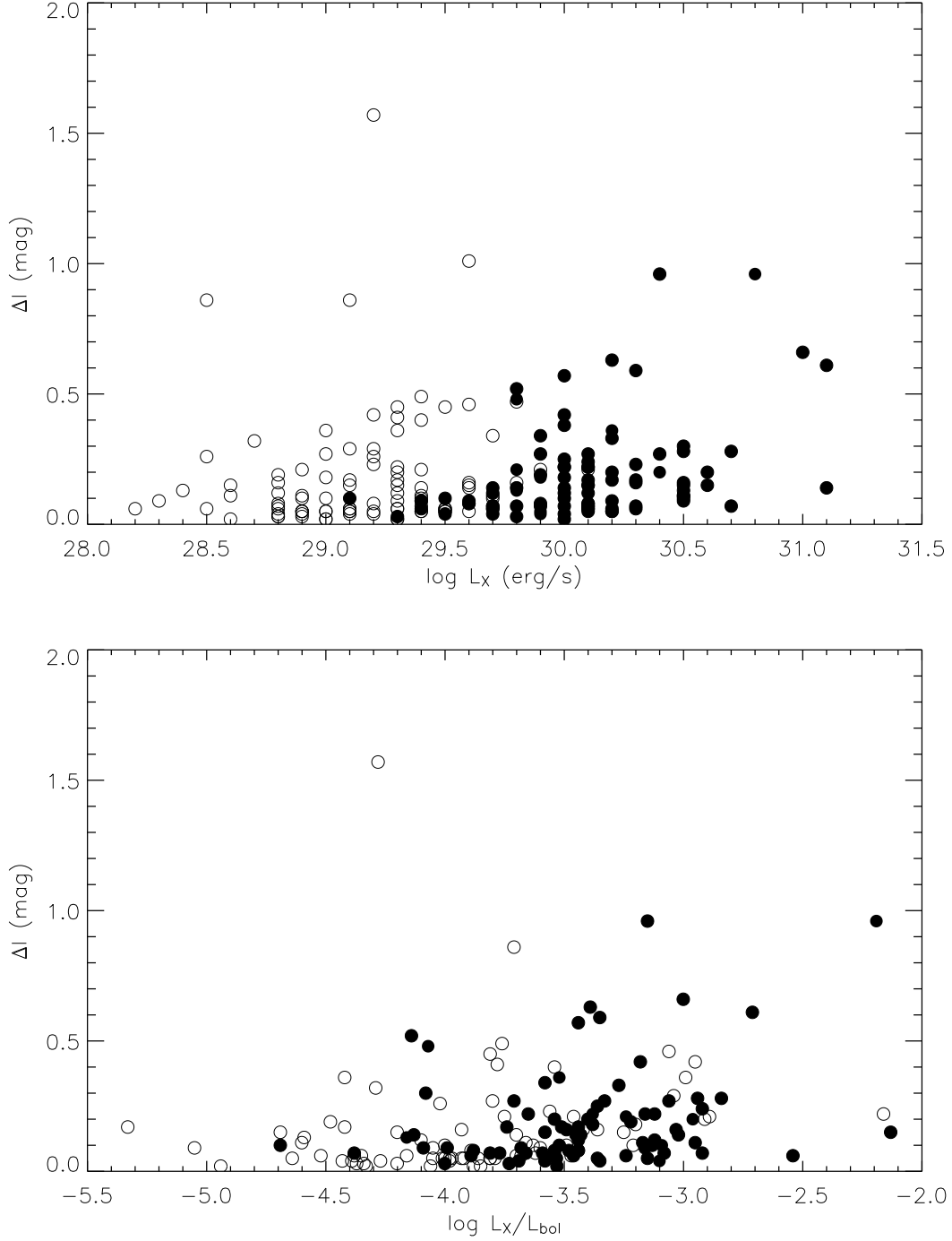


Fig. 13.— Amplitude of photometric variability in the  $I$ -band is plotted vs.  $L_X$  (top) and  $L_X/L_{bol}$  (bottom) for stars with optically determined rotation periods. Symbols are as in Fig. 8.

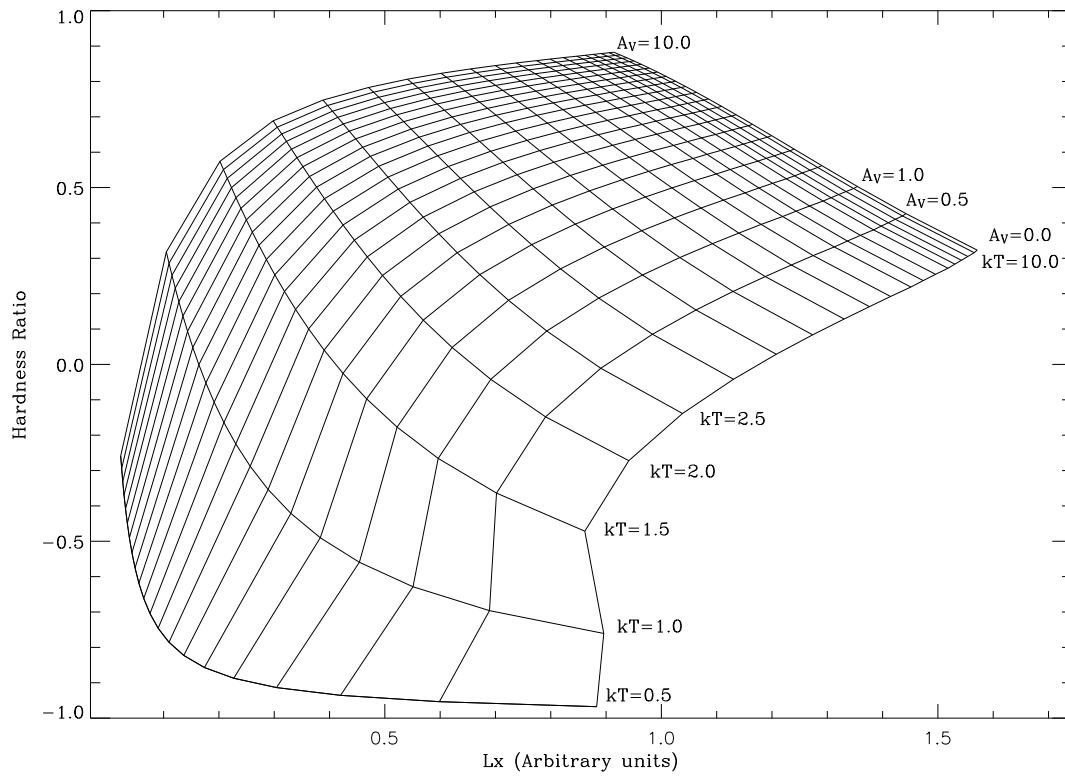


Fig. 14.— Theoretical hardness ratios as a function of  $L_x$  for different values of  $kT$  and  $A_V$ . The curves are marked with optical extinction and  $kT$  values. The abscissa values are arbitrary up to a multiplicative constant.

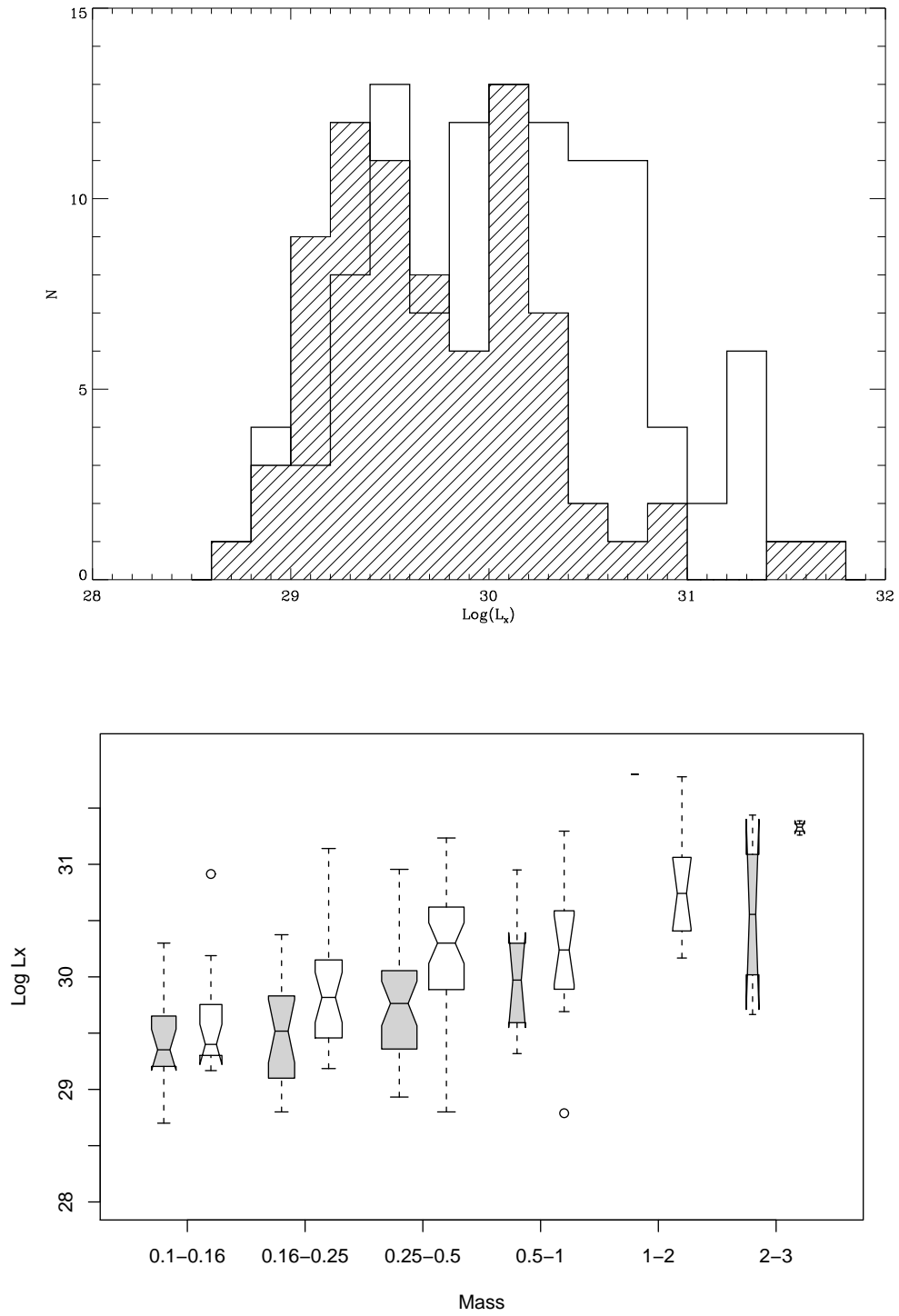


Fig. 15.— X-Ray luminosities, corrected for interstellar extinction. See Fig. 11 for an explanation of symbols. A K-S test indicates that the probability of the two histograms being drawn from the same parent distribution is  $4 \times 10^{-4}$ .

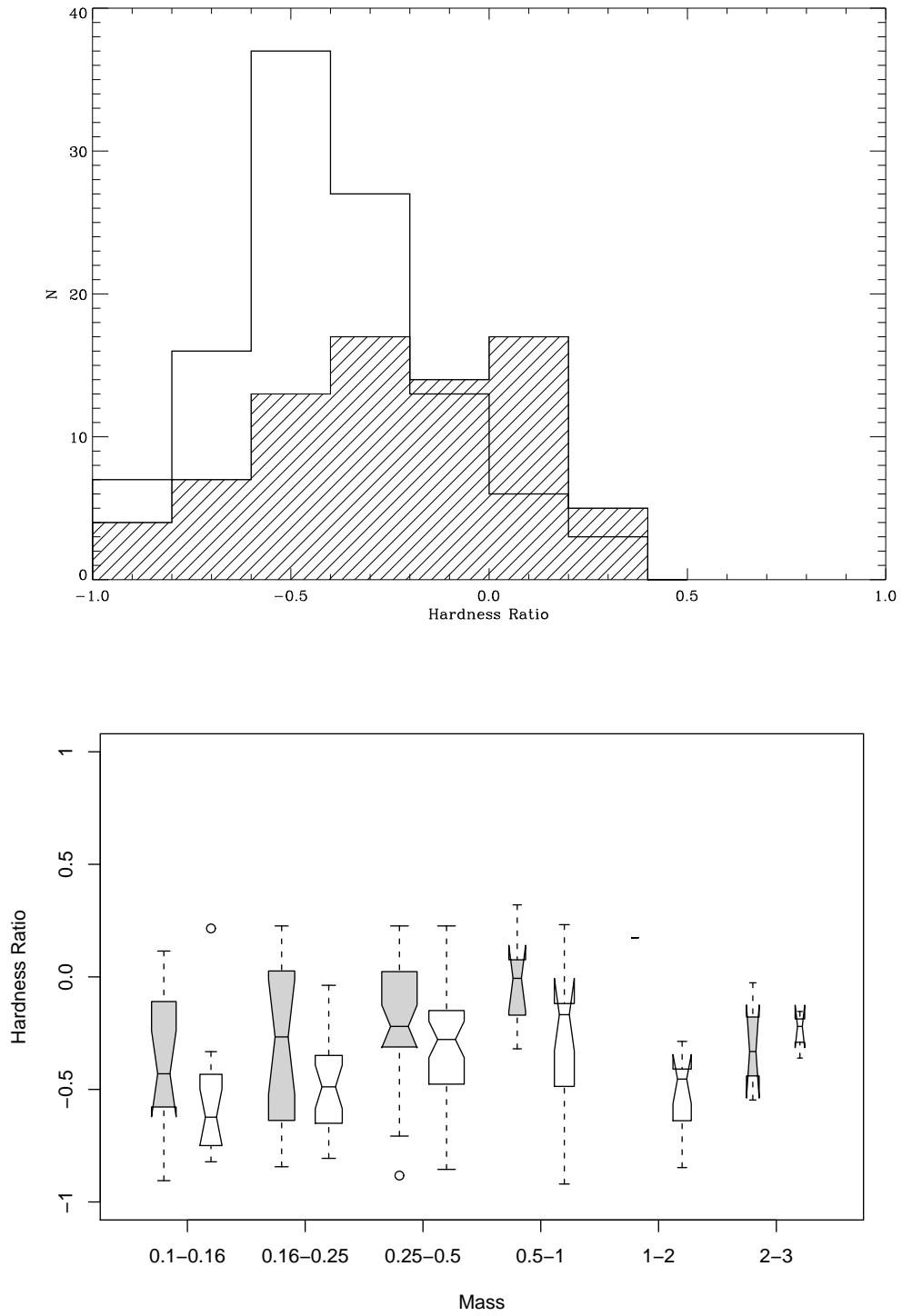


Fig. 16.— HR values, corrected for interstellar extinction. See Fig. 12 for an explanation of symbols. A K-S test indicates that the probability of the two histograms being drawn from the same parent distribution is  $2 \times 10^{-4}$ .

Table 1. Study sample

ID <sup>a</sup>	$P_{rot}$ days	$M_{\star}$ $M_{\odot}$	$\log L_{bol}/L_{\odot}$	$\Delta(I - K)$ mag	EW(Ca II) Å
106	1.70	0.21	-0.29	0.10	1.5
111	4.94	0.42	-0.15	0.24	2.2
116	2.34	0.69	0.20	0.09	1.6
118	1.07	0.13	-0.61	-0.32	0.0
122	0.98	0.14	-0.54	-0.17	0.0
123	6.63	1.37	0.28	1.28	0.0
128	8.83	0.15	0.28	0.32	0.0
133	2.03	0.29	-0.25	0.26	1.6
136	8.65	0.28	0.06	...	...
140	4.58	0.17	-0.19	-0.29	3.8

<sup>a</sup>Designation from Hillenbrand (1997).

Note. — Table 1 is available in its entirety in the electronic edition of the *Astronomical Journal*. A portion is shown here for guidance regarding its form and content.

Table 2. X-ray properties of study sample

ID <sup>a</sup>	Exposure <sup>b</sup>	$\log L_X$ <sup>c</sup> erg/s	$\log(L_X)_F$ <sup>d</sup> erg/s	Variability <sup>e</sup>	Flag <sup>f</sup>
174	G2	29.8	29.4	Const	0
175	G1	29.4	29.8	LTVar	0
175	G2	30.3	29.8	LTVar	1
177	G2	30.0	30.2	Flare	0
177	G1	30.3	30.2	Flare	1
178	T	30.1	...	PosFl	1
187	G2	30.5	30.3	Flare	1
187	G1	30.4	30.3	Flare	0
188	G2	29.5	29.7	PosFl	0
188	G1	30.6	29.7	PosFl	1

<sup>a</sup>Designation from Hillenbrand (1997).

<sup>b</sup>Source of measurement. G1: First Garmire exposure; G2: Second Garmire exposure; T: Tsujimoto exposure.

<sup>c</sup>X-ray luminosity from this study.

<sup>d</sup>X-ray luminosity from Feigelson et al. (2002).

<sup>e</sup>X-ray variability, from Feigelson et al. (2002) or from this study if source not included in Feigelson et al. (2002) study. ‘Const’ indicates a non-variable light curve, ‘Flare’ indicates a light curve with a clear flare, and ‘PosFl’ indicates a light curve that possibly includes a flare.

<sup>f</sup>Quality flag (see text). Measurements with a ‘1’ are those used in our analysis.

Note. — Table 2 is available in its entirety in the electronic edition of the *Astronomical Journal*. A portion is shown here for guidance regarding its form and content.